Effect of process variations on thermally curing polymeric materials within OEM surface treatment

Master of Science Thesis

SUSANNA DAHL
ANNIKA HANNEBÄCK

Department of Materials and Manufacturing Technology
CHALMERS UNIVERSITY OF TECHNOLOGY
Gothenburg, Sweden, 2012
Report No 79/2012

Effect of process variations on thermally curing polymeric materials within OEM surface treatment

Master´s thesis No 79/2012

Master of Science Thesis in the master degree program Materials and Nanotechnology

Department of Materials and Manufacturing Technology
CHALMERS UNIVERSITY OF TECHNOLOGY
Gothenburg, Sweden 2012

SUSANNA DAHL, ANNIKA HANNEBÄCK

Performed at: Volvo Car Corporation
Dept. 93662 TGS 1
Gothenburg, Sweden

Supervisors: Marcus Schmidt, Ph.D.
Göran Strannhage, B.Sc.
Volvo Car Corporation

Examiner: Prof. Mikael Rigdahl
Department of Materials and Manufacturing Technology
CHALMERS UNIVERSITY OF TECHNOLOGY
SE – 412 96 Gothenburg, Sweden

Effect of process variations on thermally curing
polymeric materials within OEM surface treatment
Master of Science Thesis
SUSANNA DAHL, ANNIKA HANNEBÄCK

Master´s Thesis 2012:

Department of Materials and Manufacturing Technology
Chalmers University of Technology
SE – 412 96 Gothenburg, Sweden
Telephone: +46(0)31 – 772 1000

Abstract

Poly (vinyl chloride), PVC, polybutadiene and epoxy-based materials are used as sealants, adhesives and vibration dampeners in the car body. The curing process for the materials was studied in laboratory ovens by simulating the times and temperatures from the process windows used in the car manufacturing. Process variations might occur since the cars are mass produced. Thermally induced changes should be investigated to enable quick analysis methods to predict the changes within the material. The materials were characterized by Dynamic Mechanical Thermal Analysis, DMTA, Thermal Gravimetric Analysis, TGA, Differential Scanning Calorimetry, DSC, Fourier Transform Infrared Spectroscopy, FTIR, hardness testing and colour testing. Three scenarios were investigated; target times and temperatures (normal curing, NC) , the maximum curing conditions, MC and the maximum curing conditions with additional number of re-runs, MCR. The normally cured samples were used as references. Process verification was performed for a validation of the results from oven simulations.

The sample preparation was performed to resemble the manufacturing process. Films and rods were produced by each material. The rheology of the material and glass transition temperature, T_g were determined using a temperature ramp in a DMTA rheometer. The rubbery materials were swollen in toluene for five hours in order to investigate the crosslink density.

The polybutadiene-based materials were not fully vulcanized in the NC case. The crosslinking process was continued during MC and MCR. One of the materials got surface cracks which could be a result of oxidation. The epoxy-based material increased in T_g between NC and MC. The hardness increased significantly from NC to MCR. The crosslinking can continue for a long time inside the car body and the flexibility within the material is decreased which can affect its damping properties. The PVC materials increased in T_g in the order from NC to MCR due to loss of plasticizer which decreases the flexibility of the polymer chains. This also caused a loss of damping modulus. For one of the materials used as vibration dampener and stone chips protector, the adhesion promoter migrated to the surface after the MCR scenario. The hardness increase was surface related.

Keywords
Polymer, PVC, polybutadiene, epoxy, sealants, adhesives, thermal degradation, crosslinking, DMTA and car body.

Preface

This thesis is the examination work for a Master of Science degree in Chemical engineering. The thesis has been performed at the department Surface Treatment Centre Corrosion Protection and Adhesives, at Volvo Car Corporation, VCC, Gothenburg, Sweden in collaboration with the Department of Materials and Manufacturing Technology at Chalmers University of Technology.

We wish to express our sincere thanks to our supervisors of this project, Ph.D. Marcus Schmidt and B.Sc. Göran Strannhage, for their valuable guidance and advice. This project would not have been possible without their help and contribution. Furthermore, we would like to thank Volvo Car Corporation for letting us performing our master thesis and providing us with materials and equipment. We also wish to express our appreciation to our examiner, Prof. Mikael Rigdahl for all support and valuable feedback.

In addition we would like to thank Madeleine Stoopendahl for her assistance with the analysis and useful hints. Thanks also to Giovanna Iannuzzi for helping us out with DSC. Warm thanks go to the employees at the Surface Treatment Department for their kindness and helpfulness. Special thanks to Jesper Alm for helping us with SEM, to Anders Dahllöf for helping us with the tensile testing, to Lisa Lundberg for showing us the FTIR, Magnus Jarlid for a pedagogic education of colour testing, Anders Makkonen, Roy Johansson and Dr Håkan Mattsson. We would like to show our appreciation to Håkan Svensson and all the employees at TB2 who made the process verification possible. Thanks to Arne Holmström for providing us with his experience and knowledge in polymeric chemistry. Finally an honourable mention goes to our families and friends for their understanding and support that enabled us to complete this project.

The project has been performed at Volvo Car Corporation, which is a car manufacturer earlier owned by the Swedish company Volvo AB. It was bought by Ford Motor Company in the year 1999 [1] and sold to the Chinese company Zhejiang Geely Group Holding Co. Ltd. in 2010. Li Shufu is presently the chairman of the board [2]. The company vision is: "To be the world's most progressive and desired luxury car brand". The head quarter office is located in Torslanda, Gothenburg, together with a large production site, where many of the car models are produced [2]. The department Surface Treatment Centre Corrosion Protection and Adhesive performs research and development for higher quality and improvement of the car manufacturing process.

Gothenburg, Sweden

March 2012

Susanna Dahl and Annika Hannebäck

List of contents

List of abbreviations

CIE Commission Internationale de l'Eclairage – International Commission on Illumines
DMTA Dynamic Mechanical Thermal Analysis
DSC Differential Scanning Calorimetry
FTIR Fourier Transform Infrared Spectroscopy
GC-MS Gas Chromatography-Mass Spectrometer
IRHD International Rubber Hardness Degrees
MC Maximum Curing
MCR Maximum Curing with Re-runs
NC Normal Curing
NVH Noise Vibration Harshness
OEM Original Equipment Manufacture
PVC Poly (vinyl chloride)
STC Surface Treatment Centre
SEC Size Exclusion Chromatography
SEM Scanning Electron Microscopy
TGA Thermal Gravimetric Analysis
VCBC Volvo Cars Body Components
VCC Volvo Car Corporation

1. Introduction

1.1. Background

Comfort is an important criterion when choosing car brand since people use the car for commuting [3]. To improve the comfort, polymeric materials are used in the car body to absorb vibrations and prevent fluttering in the engine hood, roof, trunk-lid and doors [4]. The vibration damping properties of a polymeric material refer to the mechanical properties and the materials ability to absorb vibration and convert it to heat. In the car body, materials based on poly (vinyl chloride), epoxy and polybutadiene are used for the anti-vibration and sound deadening purpose.

In the roof, high strength boron-steel bows are used to increase the safety in case of a collision. To avoid fluttering between the outer sheet metal and the roof-bow, polybutadiene-based material is applied. The material has high mechanical strength, adhesive properties and the ability to store energy which is important for vibration dampening.

For corrosion protection sealants are applied to hinder water and dirt to get in contact with the cavities of the car body. Materials based on PVC are used as hem flange- and roof-ditch sealants. All the parts that are applied on the car body; doors, engine hood and trunk lid have sheets that are joined together by rubbery-based hemflange adhesives. To achieve water tightness sealant is applied. The material that is used as sealant should have high resistance to water and other solvents. The weld-through sealants are polybutadiene-based, due to high resilience and low shrinking. The adhesives, sealants and sound-deadening materials are applied in the body-shop before surface treatment and painting of the car body.

By simulating times and temperatures in the ovens from the process windows, the thermal influence on the polymeric materials can be studied. Characterizations of the material properties will include both an investigation of the mechanical properties and a study of the chemical degradation and decomposition. [5] The rheology is studied by a temperature ramp in DMTA. TGA and DSC are used for investigation of thermal degradation. Other possible characterization methods are evaluated in a pre-test. The exact chemical composition of the materials is proprietary information of the suppliers. The overall compositions are given in the suppliers' technical datasheets.

The project results can be used to examine how the materials' properties change when curing times and subsequent oven times proceed longer than expected. Since cars are mass-produced it is necessary to make quick decisions during the process. Therefore there is a large interest in using indicative analysis methods that can show if the material still meets the demands. To interpret the results it is necessary to know the mechanisms controlling the thermally induced changes in the polymer materials.

The process variations are studied by performing simulations of two scenarios that can be compared with the normal and targeted curing conditions. The scenario that simulates maximum temperatures and times refers to the case when the production is delayed. The worst case scenario is maximum curing in the ovens and with additional re-runs. The re-runs are added in order to maintain the quality for all the car bodies.

1.2. Problem formulations

The car manufacturing process at VCC is a large-scale production, involving an assembly line with process windows. All car bodies passing through the ovens are not exposed to exactly the same conditions. This means that curing temperatures and times can deviate between the materials in different car bodies.

In order to characterize the properties of the cured polymers, suitable analysis methods must be considered. One disadvantage with polymers is their relative temperature instability. Degradation and decomposition may occur since the binding energies are relative low caused by weak intermolecular interactions [5]. The possible degradation mechanisms are here predicted from knowledge based on a literature study. The important properties for each material are also considered. This deeper knowledge might lead to the possibility to use rapid indicative analysis methods, for example hardness testing and colour testing.

1.2.1. Purpose

The aim of this project is to investigate how the polymeric materials change in composition and mechanical properties depending on temperatures and times within the existing process windows. By characterization of mechanical properties and chemical composition the mechanism that control thermally induced changes can be understood and controlled. The polymeric materials included in this project are from the materials portfolio at Surface Treatment Engineering at VCC.

1.3. Constraints

The interesting oven times and temperatures are within the existing temperature and time windows in the production process. The project involves only the polymeric materials that are applied on the car body before the primer surfacer. This means that all polymeric materials applied after the car body is painted are excluded in this study.

The eight materials that are investigated are of interest to the Surface Treatment Centre, S.T.C, Corrosion, Protection and Adhesives, due to its responsibility and commitment for the quality of these materials.

During the process the polymers might be covered with paint. As a result, the degradation reaction may change due to the limited exposure to air. Therefore it is not intended to cover the sealants inside and under the car body. The painting process; primer surfacer, base coat and clear coat, is excluded from this project.

The thickness of the polymeric layer could differ when the materials are applied in the process. This can affect the degree of curing in the car manufacturing. The thickness parameter is excluded from the project.

In the process the sheet metal is covered with press oil. The sheet samples were not prepared with oil in the experiments.

2. Theory

In the following chapter the investigated materials and their response to thermal treatment is described. The theory behind the analysis methods used in order to make evaluations of applied materials in the car manufacturing process is also outlined.

2.1. Polymeric materials used at VCC

2.1.1. Polybutadiene

Polybutadiene is an elastomeric polymer which is a synthetic rubber. The polymer repeating unit has a backbone of four carbon atoms with alternating double bonds, shown in Figure 1. Elastomeric materials are highly random and flexible polymer chains crosslinked at few sites, approximately one crosslink per 2000 carbon atoms. [5]

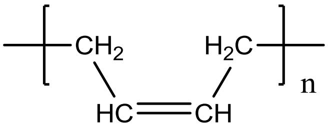

Figure 1. Polybutadiene repeating unit [5]

The main additives in elastomeric materials are; reinforcing and inactive fillers, oils, vulcanization agents, antioxidants, waxes and pigments. The vulcanization agents, accelerators, activators and retarders are involved in the crosslinking process [6]. Vulcanization is a process whereby polymer chains are crosslinked and the viscous material transforms to an elastic rubber. Vulcanization can also be called curing or crosslinking. Rubber products have high resilience which means that after a load has been removed the original dimensions are restored immediately. The three-dimensional network structure with long-chain rubbery molecules that bonds together at crosslinking points gives the elastomer its elasticity. [7]

Sulfur can be used as vulcanization agents for curing rubbers that contain unsaturations, where the sulfur creates sulfide bonds between the polymeric backbones. The final properties of the material depend on which type of vulcanization system that is used. The length of sulfur-crosslink can be controlled depending on the amount of accelerator with regard to the amount of sulfur. Larger amount of sulfur gives longer sulfide crosslinks, which increases the tensile strength. Disadvantage is decreased ageing resistance. [7]

Two forms of sulfur are used in rubber materials. One is soluble, often rhombic crystals containing eight sulfur atoms in a ring, the second is an insoluble amorphous polymeric sulfur. During heating the sulfur ring breaks down and crosslinks can be formed.

Vulcanization systems that are used for polybutadiene rubber also contain organic accelerators, activators and retarders. The start of the vulcanization can be customized to be delayed or rapid by choosing different vulcanization agents for example stabilizers and accelerators. [8]

Zinc oxide is a common activator for the crosslinking process; it forms a complex with sulfur molecules within the polysulfide chain. Di(benzothiazol-2-yl) disulphide (MBTS), shown in Figure 2, is used as an accelerator, it participates in the formation of the crosslink-precursor, which is important for accelerating the sulfur vulcanization. The exact position and nature of the zinc complexes in the accelerating step is still unknown. [9]

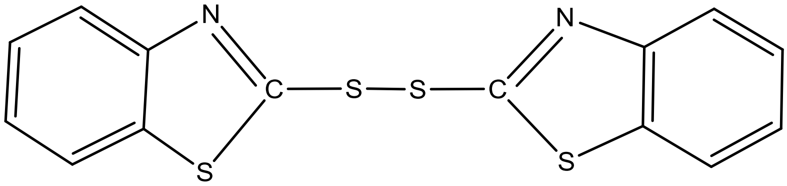

Figure 2. Accelerator of the vulcanization process, MBTS [9]

The general mechanism in the vulcanization reaction is sulfur crosslink, carbon-carbon crosslink, sulfur crosslinks of varying length and pendant accelerator sulfide.

Polybutadiene is used as adhesive and as antiflutter material in the car body. For instance, at VCBC polybutadiene based adhesives are used as weld-through adhesives in the car body and as hemflange adhesives in doors, bonnets and trunk lids. The material can also be applied in doors and on bonnets to avoid fluttering.

2.1.2. **Epoxy**

Epoxy resins are characterized by the presence of a three-member group called epoxide (epoxyethane), shown in Figure 3. The cured amorphous epoxy exhibits exceptional chemical, moisture and corrosion resistance. Epoxy provides a good mechanical strength and toughness, due to high crosslinking density [10]. The application of the polymeric material in the car body is as vibration dampener applied in the paint shop. The ability of energy storage over a large range of temperatures and frequencies is of importance in vibration damper use. [11]

For the curing process, at least two epoxide groups must be placed on each polymer chain. The reaction starts with a hardener, usually aliphatic amine, which opens the highly reactive epoxide ring. Two bonds are formed in order to crosslink the epoxy group. Between the carbon on the epoxide and the nitrogen a covalent bond is created. Simultaneously the oxygen on the epoxide group attaches to the hydrogen on the amine molecule, illustrated in Figure 4. For the crosslinking the carbon-amine bond is important. The bonding ability of the epoxy resin depends on the hydrogen-oxygen bond. [5]

The hardener molecule has two reactive sites, which means that two chain bonds to the same amine molecule. For the final cured epoxy the relative concentrations of the epoxy and the hardener are important. If the concentration of epoxide groups corresponds to the concentration of the reactive hardener the material will achieve high tensile strength and increased hardness which indicate a high density of crosslinks. [5]

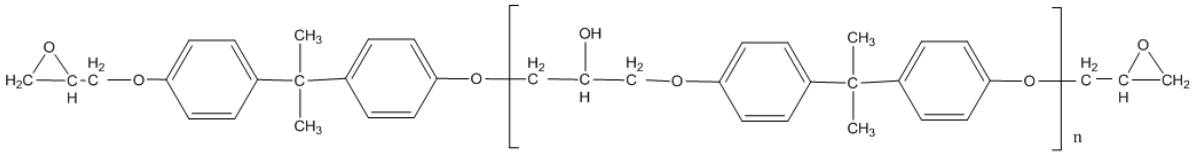

Figure 3. Epoxy resin of Bisphenol-A repeating unit connected with epoxy groups [5]

The epoxide ring opening mechanism is shown in Figure 4. The curing rate depends on the reactivity of the nucleophilic nitrogen and the temperature. The pathway is an S_N2 reaction which implies that there is a nucleophilic attack on the electrophilic center, the epoxide group. This results in a one step reaction. [12]

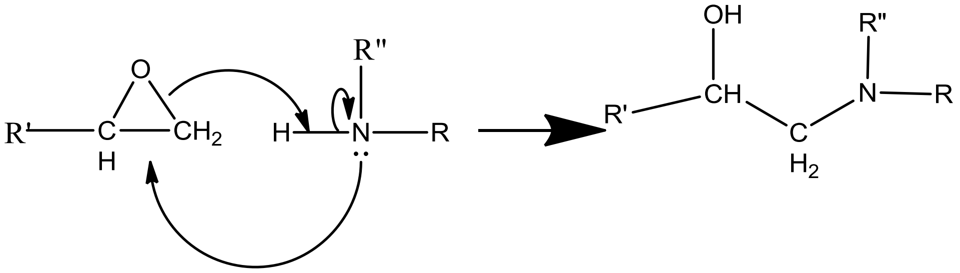

Figure 4. The reactive epoxide group reacts with the amine derivate [5]

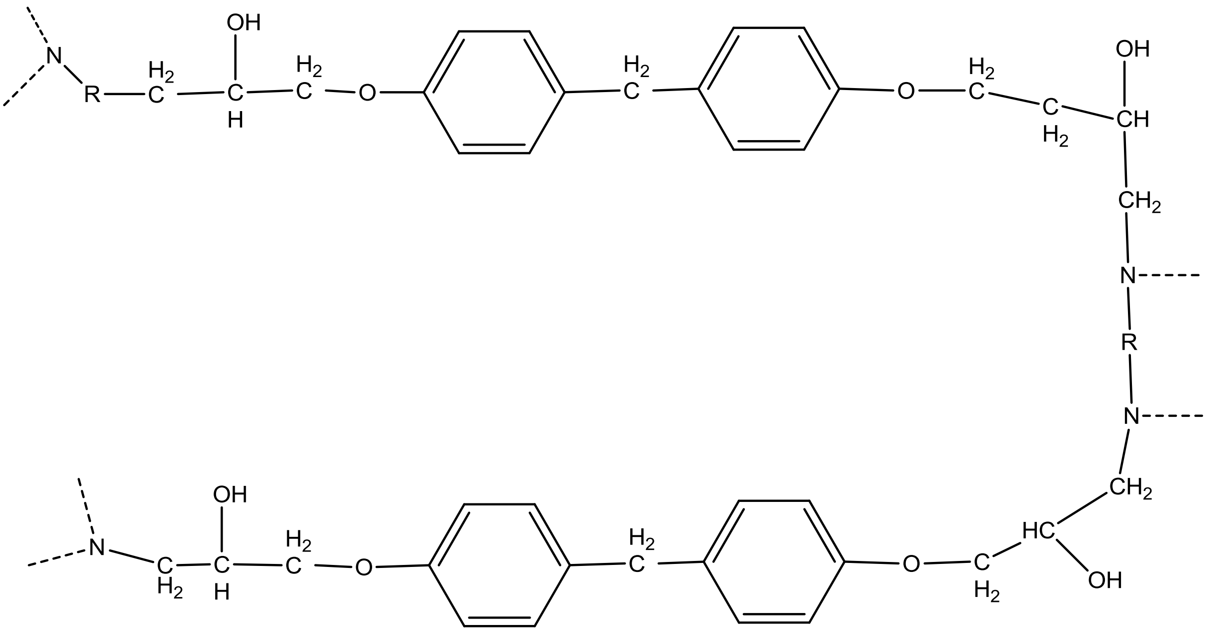

Figure 5. Curing process for epoxy, crosslinking with the amine derivate group[5]

An epoxy material with a shorter polymer backbone has a higher crosslink density. When the crosslink density increases the material gets stronger and stiffer which increases the maximum usage temperature and provides a higher resistance against solvents and chemicals. [5]

2.1.3. **Poly (vinyl chloride), PVC**

PVC is a common thermoplastic polymer. The monomer is a double-bonded carbon with a chlorine atom and hydrogen atoms which is polymerized using the addition (free radical) polymerization method; the repeating unit is illustrated in Figure 6. The chlorine atom provides significant properties. It prevents close packing and induces a solvent sensitivity because of the high electron negativity. Unmodified PVC is called rigid PVC and as a solvent modified, plasticized PVC. The plasticized PVC are much more flexible since the plasticizer acts as a poor solvent for the plastics and causes disentangling of the molecules, swelling of the material, and some breaking of secondary intermolecular bonds. It reduces the brittleness and rigidity and therefore induces a decrease in tensile strength. The glass transition temperature, T_g is reduced which makes it rubbery at room temperature.[12]

There is a processing method which does not require melting of the temperature sensitive plastic. Instead PVC powder is suspended in a plasticizer which increases processability. The suspension is called a plastisol. During curing of the PVC the plasticizer forms a gel with the polymer, caused by molecular entanglements and hydrogen bonding. [12]

The PVC based materials are used as sealants, abrasion protection and as vibration dampeners in cars. It covers flanges to provide corrosion protection and cushioning. The exact composition of the materials is confidential from the supplier but they contain plasticizers, fillers, stabilizers and adhesive promoter. The solvent used for the investigated materials is dearomatized petroleum naphtha. A commonly used plasticizer is diisononyl phthalate (DINP), shown in Figure 7. [5]

For plastisol used as corrosion protection an important quality criterion is the adhesion to the coated surfaces. The risk of penetration of corroding fluids increases when the adhesion of the protective layer is relatively low. When a PVC-based material is used as a protective layer, an adhesion promoter often is added. The promoter has the function to bring long lasting adhesion to the electro coated surface. Polyaminoamide is a commonly used adhesive promoter. A disadvantage in using free polyamines for increased adhesion is that pale, white or pastel coloured coatings discolour during curing. [13]

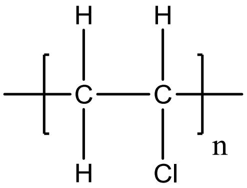

Figure 6. Chemical structure of PVC repeating unit [5]

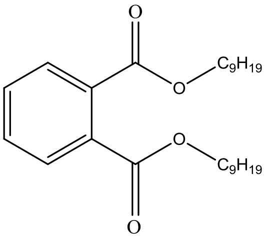

Figure 7. DINP plasticizer used in PVC

2.2. Thermal degradation and decomposition mechanisms of polymers

The difference between the terms degradation and decomposition, is that during thermal degradation the heat causes a loss of physical, mechanical or electrical properties. In thermal decomposition the material combusts and generates fuel vapors. For polymeric materials these two mechanisms can occur simultaneously during a thermal treatment and they are therefore difficult to distinguish. [14]

The change in physical properties of a polymer during heating differs between thermoplastics, thermosets and elastomers. Heating of a thermoplastic makes it softer and it eventually melts, while thermosets are infusible. Thermosets have often a higher softening temperature and will not melt, instead it degrades thermally, see Figure 8. For elastomers the crosslinking may continue, the material loses its flexibility and finally it degrades. The thermal decomposition of polymers may proceed by oxidative processes or simple by the action of heat, often accelerated by oxidants. [14]

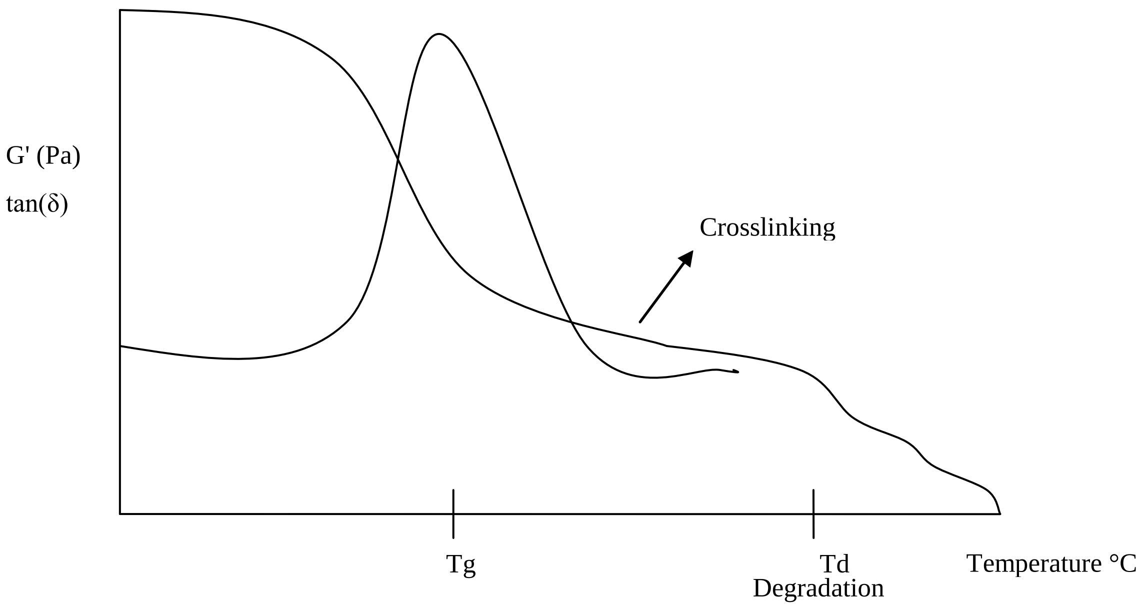

Figure 8. A general graph describing the modulus of a thermosets as a function of temperature, the maximum damping is the materials T_g. Higher crosslinking density increases T_g. After the degradation temperature of the material, T_d the material start to degrade in several steps with increasing temperature. T_g depends on free volume, intermolecular forces and chain flexibility.

The three major pathways that can take place during thermal degradation of polymers are side group elimination, random scission and depolymerisation. During the depolymerisation process, the end of the polymer chain leaves and forms a low molecular weight free radical, the chain reaction mechanism causes loss of monomers. The random chain scission breaks down the backbone randomly which causes a decrease in molecular weight. Side groups are connected to the polymer backbone with weaker bonds than the bonds connected within the polymer backbone, which results in stripping of side groups at lower temperatures. Thermal degradation involves changes in molecular weight of the polymer and typical property changes include reduced ductility, embrittlement, colour changes and cracking. [15]

The general mechanisms of thermal decomposition include random chain scission, end chain scission, chain-stripping, crosslinking and side chain cyclization. Crosslinking can be indicated by an increase in glass transition temperature and tensile strength.

Thermal degradation governs the upper limit for the polymer processing temperature. The materials can contain thermal stabilizers which react with the available free radicals to produce less reactive free radicals and slow down the degradation process. The degradation mechanisms may involve an auto oxidation process, which includes the depolymerizing steps initiation, propagation, branching and termination.[16]

2.2.1. **Thermal degradation of polybutadiene**

Thermal degradation of polybutadiene yields crosslinks along the polymer chain. The polymeric material shrinks, becomes harder and the flexibility decreases. Oxidation of the polybutadiene can also cause chain-scission which softens the elastomer, which is a common reaction for natural rubber. The types of crosslinks formed during vulcanization affect the thermal stability of the material. If the crosslinks are dominated by monosulfidic linkages it has a higher stability than the polysulfidic links. This is attributed by higher dissociation energy of C-S bonds compared to S-S bonds. [17] Cyclization can occur in the product. Decomposition at 798 ˚C in air gives a dark impermeable crust, which hinder further contact with air.

2.2.2. **Thermal degradation of epoxy**

Epoxies are usually blended with elastomers in order to improve toughness, due to this blending the thermal stability is also improved. The curing agent has a great influence of the thermal stability. Epoxy resins cured with amine are stable due to the nucleophilic nature of the amine. [18] A possible mechanism at low temperatures is hemolytic chain scission which leads to cleavage of covalent bonds. Other possibilities are recombination of radicals formed by degradation causing crosslinking and randomizing of its structure. The first mass loss is a result of dehydration due to elimination of water from the propylene group and subsequent formation of double bonds. The products from the scission of the polymeric chain yield unsaturated phenolic compounds which produce a char. Incompletely cured epoxy resin and resulting free functional groups, have an influence on the thermal stability. They can act as the centre of polymer chain scission. The thermal stability is improved with the degree of crosslinking. At lower temperatures the degradation mechanisms are not atmosphere dependent. [18] The degradation reaction proceeds through several concurrent pathways for example cleavage of bisphenol-A to yield isopropylphenol, ethylphenols, cresols and phenol [19].

2.2.3. **Thermal degradation of PVC**

PVC has relatively low thermal stability and becomes degraded when thermally exposed. During degradation, hydrochloric acid gas is produced and double bonds form among the polymer chains, illustrated in Figure 9. To avoid release of hydrochloric acid, which can cause local corrosion, stabilizers are added and the hydrochloride acid can also bind to added calcium minerals which are used as fillers in PVC materials. The crosslinking that occurs between chains results in a fully carbonized residue at higher temperatures. During thermal degradation the colour first switches to yellow and later to brown. The presence of oxygen accelerates the dehydrochlorination process, which causes main chain scissions and reduces crosslinking. When the process starts, other nearby chlorine and hydrogen atoms combine and accelerate the decomposition, so called autocatalytic decomposition. Thermal stabilizers are added to avoid degradation mechanisms within the PVC material. [5]

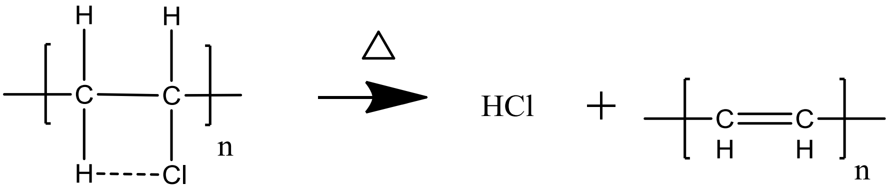

Figure 9. Dehydrochlorination process of PVC [5]

2.3. **Experimental techniques**

2.3.1. **Dynamic Mechanical Temperature Analysis, DMTA**

Rheology is the science that deals with the deformation and flow of materials in the solid, liquid or molten state in terms of elastic and viscous properties of the material. In Dynamic Mechanical Temperature Analysis, DMTA, a sinusoidal deformation is applied to a sample at a specified frequency and the viscoelastic response of the deformation (i.e. stress) is measured, see Figure 10. In order to use DMTA, the response of the material should be independent of the magnitude of deformation and the structure within the material shall remain intact. The material must thus be deformed at a strain that is within the linear viscoelastic region. The linear region for each material can be estimated by performing a strain- sweep test. [20]

DMTA makes it possible to determine the viscoelastic properties of a polymer as a function of time, temperature and frequency. Adhesives and sealants are polymeric materials so they have both viscous and elastic properties, thus they are viscoelastic. A sample with a rectangular shape is attached between two clamps. A small sinusoidal strain, Eqn 1, is imposed on the sample and the resulting torque or force is measured, which refers to Eqn 2 [20], see Figure 10. Properties that can be determined corresponds to the rheological fingerprint of the material and they are phase shift, glass transition temperature, yield stress, viscosity, storage modulus G' and loss modulus G".

Input strain wave: $\epsilon = \epsilon_{\mathbf{0}} \sin(\omega t)$ (1)
Output stress wave: $\sigma = \sigma_0 \sin(\omega t + \delta)$ (2)

$\epsilon = \text{strain}$
$\epsilon_0 = \text{strain amplitude}$
$\sigma = \text{stress}$
$\sigma_0 = \text{stress amplitude}$
ω = frequency
t = time
δ = phase shift between stress and strain

G' is called the storage modulus and is a measure of the periodic storage and release of energy in the sinusoidal deformation process, described in Eqn 4. G' is defined by the materials specific ability to store strain energy. G", the loss modulus, is a measure of the energy dissipated as thermal energy or in a sense used in molecular rearrangements in the same deformation process, described by Eqn 5. The complex modulus, G^*, is defined as the materials ability to withstand deformation, Eqn 3. For completely elastic materials the phase angle δ is zero, for viscous materials δ is 90°. Tan δ, described in Eqn 6, is a measure of the damping in the material. [20]

Complex modulus: $G^* = \frac{\sigma}{\epsilon} = G' + iG''$ (3)
Storage modulus: $G' = G^* \cos\delta$ (4)
Loss modulus: $G'' = G^* \sin\delta$ (5)
Damping factor: $\tan\delta = \frac{G''}{G'}$ (6)

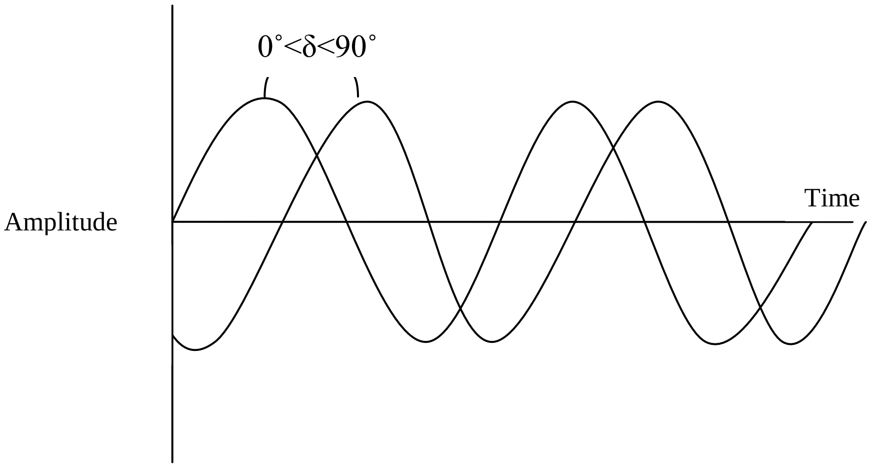

Figure 10. Illustrating a phase shift of oscillating response [11]

2.3.2. Thermogravimetric Analysis, TGA

Thermogravimetric analysis monitors the mass change of a material that is subjected to a controlled temperature ramp within atmospheric environment. The mass change is a function of time and temperature. By comparing mass changes at certain temperatures for different polymeric materials the thermal stability can be estimated [21]. The mass change can also be associated with degradation processes and volatile groups. The change of mass is recorded by a sensitive balance. The remaining ash content is received if the sample is combusted in air during the analysis. The thermo balance can measure with a 0,1 µg precision and standard masses are used for calibration. The sample can be heated up to 2800 ˚C with a heating rate that can be varied from 0,1 to 300 ˚C/min. Nitrogen, argon, helium or oxygen atmosphere can be used for studying different reactions. [21]

2.3.3. Differential Scanning Calorimetry, DSC

DSC can be used to determine the rate and degree of heat change as a function of time and temperature. Different thermal properties, for example T_g and other phase transitions, can be investigated in organic and inorganic materials. The sample and a reference sample are exposed to the same temperature ramp, the different amount of heat required to keep the sample and the reference at the same temperature is measured as a function of temperature. During phase transitions within the sample more or less heat will be needed to maintain the same temperature as the reference sample. For exothermic reactions less heat is needed and for endothermic reactions more heat is needed. The glass transition temperature T_g refers to the second-order heat-capacity change in the polymer. [21]

2.3.4. Fourier Transform Infrared Spectroscopy, FTIR

FTIR is a method to characterize the composition of an unknown material by sending light in the infrared spectrum through (or towards) the sample and measure the absorption or by collecting the reflected light. The chemical bonds interact with the light at certain frequencies corresponding to the specific type of bonds and the included elements. It is only possible to detect molecules with a dipolar of induced moment. The specific energy needed to excite the bond corresponds to the energy of a specific wavelength of light.

By measuring the amount of light absorbed by the sample at certain wavelengths it is possible to characterize and quantify the bonds between the atoms. The data is presented in a spectrum and can be used to determine the functional groups of the compounds.

2.3.5. **Colour testing (colourimetry)**

When the visible region of the electromagnetic spectrum illuminates a sample it interacts with the atoms and molecules within the material. The material absorbs light at specific energy and the reflected energy appears as a colour in the human eye.

A spectrophotometer was used to measure the ratio between the reflected and the incident light. The ratio is measured for a sample at many points across the visible spectrum. The reflectance, often expressed in percentage, is somewhat simplified given by Eqn 7. [22]

$$Reflectance = \frac{Reflected\ light\ intensity}{Incident\ beam\ intensity} \tag{7}$$

A spectrophotometer that measures colour is based on colour concepts. A specific illumination and viewing geometry is used to illuminate and observe the sample. The reflected light is investigated by the spectral analyzer. The analyzer splits up the light into its spectral components. The spectrophotometer can measure the spectral intensity distribution and calculate the X,Y and Z tristimulus values.

The International Commission of Illumination, CIE system is used to show how the colour is reproduced by a mixture of three light sources. The three-dimensional character of colour can be described in various ways. The non-linear transformation of XYZ to L* a* b* coordinates is called CIELAB colour space [23]. The CIELAB coordinates can be calculated from the received samples tristimulus values in relation to standardized tristimulus values. For the transformation of reflectance values to CIELAB values the standard illuminant used was D_{65} which refers to 6500 K in colour temperature and represent the daylight conditions. The 10° standard observer (CIE 1964) (which represent the human's range of visible colours) was used for all CIELAB calculations.

The lightness of the sample is described by L*, based on the scale 100 for white colour and zero for black, Eqn 8. For the a* axis, the value refers to its position between red and green, whereas b* refers to the position between blue and yellow, Eqn 9, Eqn 10. The colour axis system is based on the fact that the colour red and green, or blue and yellow, opposes each other, see Figure 11. The colour differences can be approximated by treating each colour as a point in a three dimensional space and calculate the distance between them, Eqn 11. [22]

$$L^* = 116\left(\frac{Y}{Y_n}\right)^{\frac{1}{3}} - 16 \tag{8}$$

$$a^* = 500\left[\left(\frac{X}{X_n}\right)^{\frac{1}{3}} - \left(\frac{Y}{Y_n}\right)^{\frac{1}{3}}\right] \tag{9}$$

$$b^* = 200\left[\left(\frac{Y}{Y_n}\right)^{\frac{1}{3}} - \left(\frac{Z}{Z_n}\right)^{\frac{1}{3}}\right] \tag{10}$$

$$dE = \sqrt{dL^2 + da^2 + db^2} \tag{11}$$

X_n, Y_n and Z_n are the tristimulus values for a standard illuminant and observer for a sample reflecting 100% of the light at all wavelengths. The method can be used to describe a visual colour difference, since CIELAB is designed to approximate human vision.

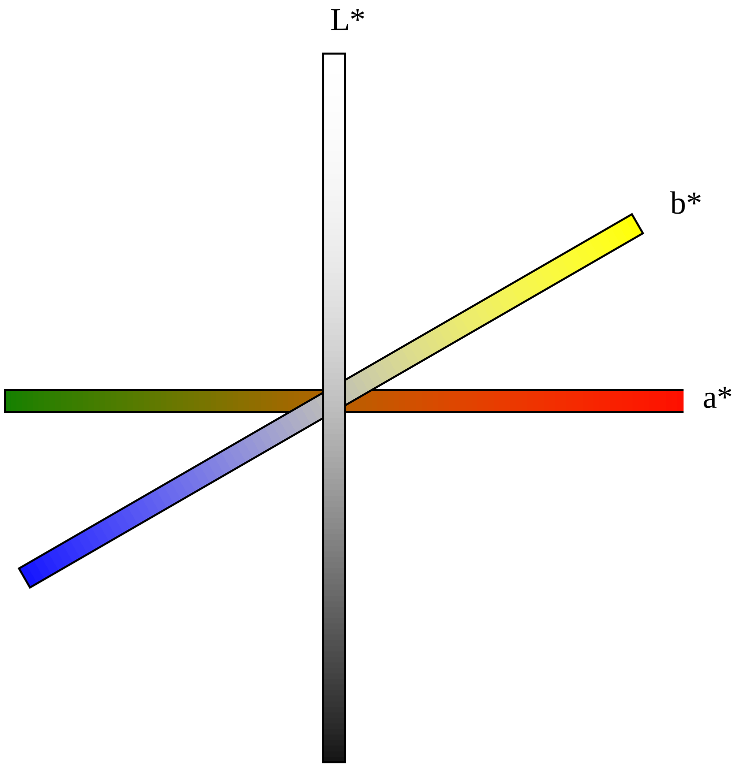

Figure 11. Illustration of the CIELAB colour system

The total colour difference (dE) can be used as a simplified description and is calculated as the geometrical sum of dL, da and db. This calculation does not take into account the varying sensitivity of human perception to colour differences in L, a and b dimensions but can still be used as a simple comparison. This calculation can be carried out for each of the five measurement angles 15 to 110° of the spectrophotometer used.

2.3.6. **Hardness testing**

The Shore Durometer or Rockwell hardness test is used to assess the material resistance against indentation. For softer plastics Shore A scale can be used and for harder plastics Shore D scale is preferred. The durometer indenter is applied with a certain force on the sample surface and the hardness is proportional towards the depth of penetration. If the penetration is total the hardness is zero and the hardness is 100 if no penetration occurs. Rubbers and plastics often exhibit resilience which means that hardness reading can change over time. This means that the loading time is important. [24]

International Rubbery Hardness Degree, IRHD, is another scale for measuring hardness of rubbers. The spherical indenter of the instrument indents the sample under a minor and major load. The resulting IRHD value refers to the differential indentation depth. [25]

2.3.7. **Swelling of polybutadiene**

From swelling in liquids, the crosslink density can be calculated. The crosslinked elastomeric material is not dissolved; it absorbs the solvent and swells. The swelling process continues until a steady state is reached. Then the retractive forces within the extended molecular network are in balance with the forces that tend to swell the network. To relate the amount of swelling to the crosslink density, the Flory-Rehner equation is widely used, Eqn 12. The equation is valid for unfilled elastomeric materials.

$$N' = -\frac{1}{2V_s}\frac{\ln(1-\nu_r)+\nu_r+\chi\nu_r}{\nu_r{}^{1/3}-{}^{\nu_r}/_2} \tag{12}$$

where N' is the number of molecules per unit volume, V_s is the molar volume of the swelling solvent. The volume fraction of rubber in the swollen gel is ν_r and χ is the interaction parameter between the polymer and solvent. For elastomers containing carbon black as reinforcing filler ν_r can be calculated from the Kraus expression, Eqn 13.

$$\frac{\nu_r}{\nu_{rf}} = 1-\left\{3c\left[1-\nu_r{}^{1/3}\right]+\nu_r-1\right\}\frac{\theta}{1-\theta} \tag{13}$$

where ν_{rf} describes the volume fraction of filled rubber in the swollen gel, c is the filler-rubber interaction parameter and θ is the volume fraction of filler in the unswollen filler rubber [26]. The correlation between crosslink density and the swelling ability of the polybutadiene is used to investigate the degree of curing. Increased crosslink density corresponds to decreased ability to absorb the solvent. This phenomenon is here used in a simplified form, where the increased length is correlated to the ability to absorb solvent, in other words the crosslinking density. Higher crosslink density corresponds to a lower solvent absorption, which implies a smaller increase in length. For polybutadiene, toluene is a common solvent for swelling measurement. Toluene is a nonpolar organic solvent which has an interaction parameter of 0,31 - 0,47 [26] with polybutadiene.

3. Experiments

In the following chapter the experimental part is described. The manufacturing process and the investigated material are presented to obtain an understanding of the experimental work involving the oven simulations and curing conditions. The procedures for the characterization methods are described. To estimate the oven simulation reliability, a process verification was performed.

3.1. Materials

The investigated materials are listed in Table 1. The materials are applied in the car manufacturing process at VCC, Torslanda and VCBC, Olofström. All materials contain calcium oxide, CaO, which is used as water scavenger, Eqn 14, to avoid blisters in the material during curing. The pigment releases water during the curing process. The application areas are illustrated in Figures 12-14.

$$CaO + H_2O \rightarrow Ca(OH)_2 \qquad (14)$$

Table 1. The composition, application and properties of the used materials

	Polymeric material	**Application**	**Additives**	**Properties (25°C)**	**Colour**
E1	Polybutadiene	Antiflutter, hem flange adhesive for trunk-lid and engine hood	MBTS, ZnO, CaO in oil,	Soft and elastic	Yellow
E2	Polybutadiene	Weld-through sealant for the car body	MBTS, ZnO, CaO in oil	Soft and elastic	Black
E3	Polybutadiene	Hem-flange adhesive	MBTS, ZnO, CaO in oil	Hard and stiff	Black
E4	Epoxy	Vibration dampener, adhesive	CaO, Graphite	Hard and stiff	Black
B1	PVC	NVH and stone chips protection	CaO, naphtha	Hard	Brown
B2	PVC	Roof-ditch sealant	CaO, naphtha	Soft	Grey
B3	PVC	Flange sealant	CaO, naphtha	Soft and elastic	Yellow
B4	PVC	Roof-hatch fold adhesive and antiflutter	Epoxy resin, ZnO, CaO, resorcinol, methenamine	Soft	Pink

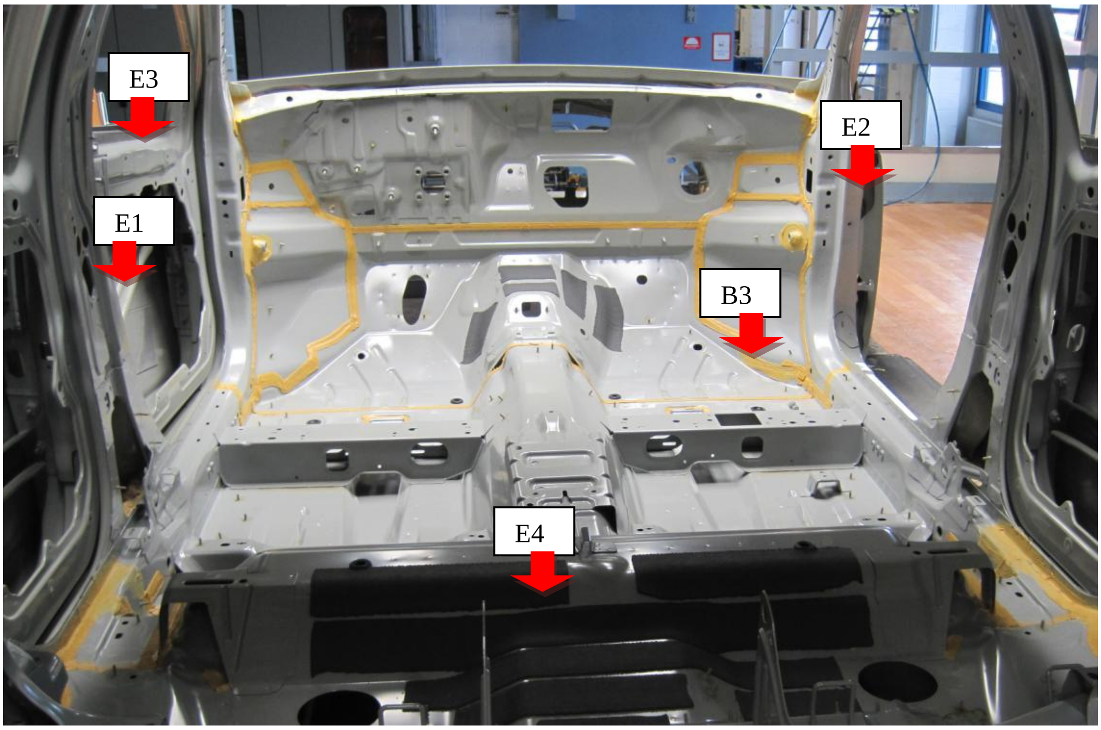

Figure 12. The inside of a car body illustrating the applied materials. E1 is an antiflutter in the hang on parts. E2 is used as a weld-through sealant in the car body. E3 is used as a hemflange adhesive in doors. E4 is the epoxy-based material used as a vibration dampener.

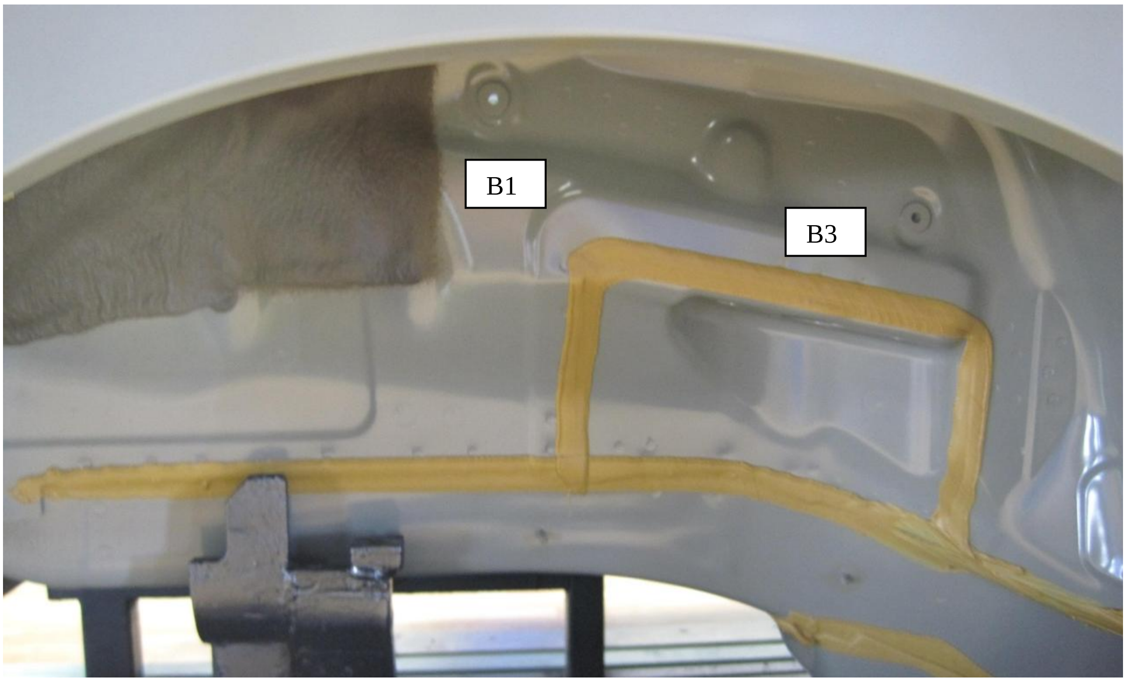

Figure 13. Picture of the wheel house illustrating the position of B1 and B3.

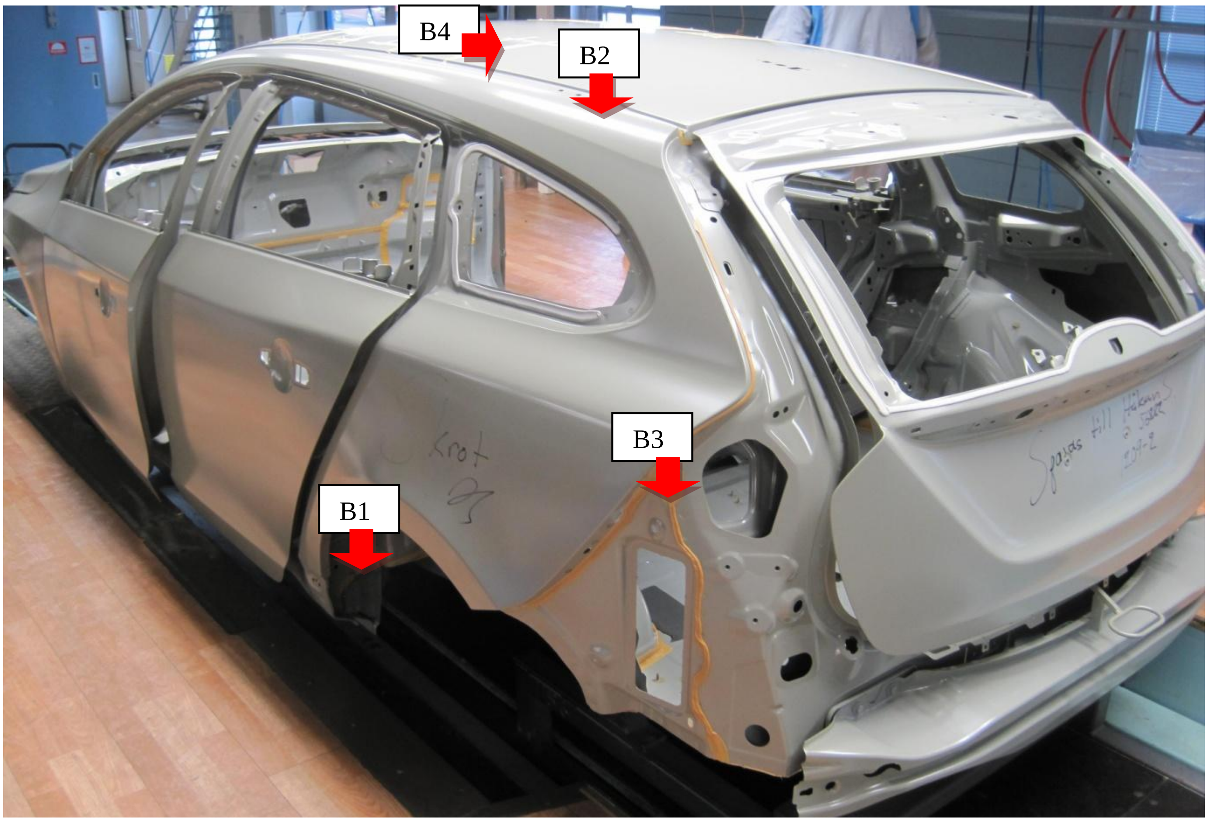

Figure 14. The car body with the applied adhesives and sealants. B1 is used as a vibration dampener in the wheel house and under the car body. The roof ditch sealer B2 is in the laser weld between the roof and the sides. B4 is used to keep reinforcement in roof hatch.

3.2.Description of the car manufacturing process

3.2.1. VCC, Body shop

The manufacturing process for the car body starts at the body shop. The steel used in the car body is pre-treated with anti-corrosion oil, applied at the mill for protection during transportation. The steel is washed and since very high forces are required during stamping, press oil is applied. The car body parts are produced by a series of different expanding dies, where the steel is cut to size and stamped into shape in several steps. Using dies in series is necessary for avoiding cracks and tensions in the material. The dies are specific for each car model.

The next step of the process involves the application of sealants and adhesives. This is achieved by using hand-operated or robotic systems. Sealants are applied to protect against ingress of water, salt and dirt. Adhesives join the body parts together and therefore have an excellent adhesion to a large number of substrates, coated with oil.

In order to prevent vibration between inner and outer panels, antiflutter, is applied under the roof and inside the engine hood and doors. Weld-through sealants are polybutadiene-based materials, which are applied on panels prior to spot welding. The material seals the joints between spot welds. Robots weld the parts together with electric current between two copper electrodes. In the roof hatch, PVC-based material is used as a hemflange adhesive for the frame reinforcement.

3.2.2. **VCBC**

The hang-on parts trunk-lid, engine hood and doors are manufactured in Olofström. The parts are produced in a similar way as the rest of the car body. Hemflange adhesive is used for filling of joints and as sealants. Antiflutter is applied in the trunk-lid, engine hood and doors. The parts are pre-cured within the target conditions, 12 min at 165°C, in an oven to maintain the quality and shape during transportation, see Figure 15.

3.2.3. **VCC, TP**

The hang-on parts are assembled on the car body which is transferred to the paint shop. The car body is washed with high-pressure jets of cleaning solution to remove oil and dirt from the panels. It is immersed in several baths with water and degreasing agents. Then it is treated with zinc phosphate for anti-corrosion and further washed. The car bodies dry at room temperature before proceeding through the electrocoat (EC) surface treatment. The electro coat is applied and cured together with body shops adhesives and sealants at 180°C for 20 minutes, target conditions, shown in Figure 15.

Paint shop sealants and adhesives are then applied to the car body for vibration damping, sealing of panel junctions and as Noise Vibration Harshness, NVH. A PVC-based material is used as flange sealants in the car body. An epoxy based material is used where high vibration dampening is required. Roof-ditch sealant is applied over a laser weld between the side panels of the body and the roof. It protects the underlying metal from corrosion and is based on a low viscosity PVC organosol. These materials are cured in the sealer/NVH oven for 17 minutes at 150 °C.

The car body is washed and dried at 120 °C for 10 minutes in oven before it is covered with a primer surfacer. It passes then an additional oven for 20 minutes at 165 °C. Then it is washed and dried for 10 minutes at 120 °C and painted with a base coat. The base coat needs to be cured in a oven for 6 minutes at 65 °C. After the top coat is applied the car body is finally cured for 21 minutes at 140 °C. The car body is then transferred to the assembly shop where additional parts are applied to complete the car. The oven temperatures and times are the target values. For the complete manufacturing process see Figure 15.

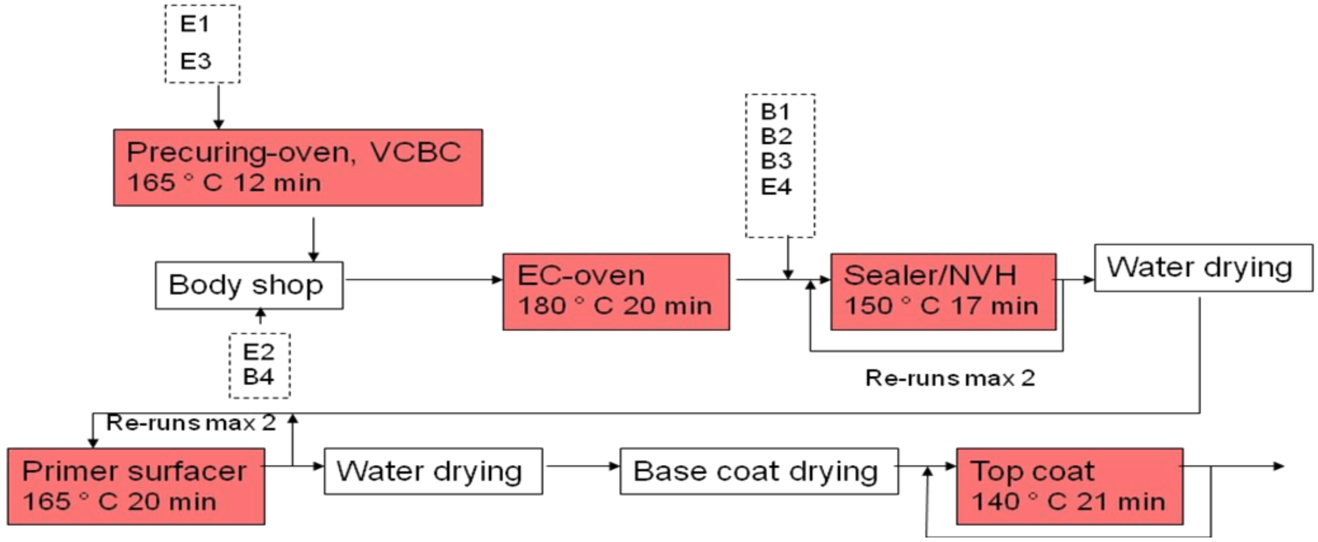

Figure 15. Schematic overview of the ovens used in the process. A description of where the materials are applied in the process, the target temperatures and times are also shown.

3.3. **Pre-test**

In order to make an evaluation of the analysis methods a pre-test was performed. Two samples of polybutadiene, PVC- and epoxy-based materials were cured for 20 minutes at 180 °C and one of each was additionally cured for 30 minutes at 180 °C. The possibility to see changes in the materials with the intended analysis methods was evaluated. The tensile strength measurements were rejected due to difficulties in measurements and production of proper samples giving adequate repeatability. Gas Chromatography-Mass Spectrometer was dismissed due to a time-consuming sample preparation and complications in dissolving the polymeric material. FTIR did not show any changes in the absorption spectrum for the PVC and epoxy materials. For polybutadiene some variation of absorbance was detected. Inhomogeneities in the materials obstruct the possibility to use SEM. SEM is also a time-consuming method and did not show any significant thermal induced changes. Colour changes and increased hardness were noticed for all the materials with the different curing times.

3.4. **Sample preparation**

The samples were prepared to suit the experimental methods and to resemble the process conditions. For DMTA, rectangular rods with a thickness depending on the rigidity were produced. These rods can be used for FTIR and hardness testing. For some of the softer PVC materials, thicker samples must be produced for DMTA analysis to achieve a stable torque signal. The mould for producing the samples was made of Teflon to avoid undesired adhesion. The materials were also applied on a steel panel covered with zinc. After the curing process, approximately one millimeter film can be removed and used for analysis. The hardness testing requires a samples thickness of about two millimeters. TGA and DSC only require a small amount of sample about 10 mg. For repeatability triplets of each sample were produced according to VCC standard testing. The weld-through sealants are not in contact with air during the car manufacturing process that involves the materials E1, E2, E3 and B4. With the intention to simulate the environment between two panels the samples were covered with aluminium foil during curing.

3.5. **Oven simulation process**

The oven process was simulated according to the existing process windows used in VCC factories in Torslanda and VCBC in Olofström.

First the target temperatures and times were simulated for normal curing, NC, according to Table 2. All the samples were cured in the oven in the given order. Different materials were heated in different ovens within the car body manufacturing processes according to Figure 15. A temperature sensor was applied on the panel and the timer was started when the substrate was 3°C below target value according to the process window. After each oven the samples were air cooled to room temperature before the next curing step. The next series of experiments refer to maximum curing, MC, temperatures and times used in the process as shown in Table 3. The maximum temperatures and times were also used in the third experiment. The difference was that re-runs were added for the ovens; sealer/NVH, primer surfacer and top coat. This procedure is called MCR.

Table 2. Normal curing conditions for simulating the process

Material	Pre.cur VCBC [°C/min]	EC [°C/min]	Sealer/NVH [°C/min]	Water Drying [°C/min]	Primer Surf. [°C/min]	Water drying [°C/min]	Base coat drying [°C/min]	Top coat [°C/min]
E1	165 / 12	180 / 20	150 / 17	120 / 10	165 / 20	120 / 10	65 / 6	140 / 21
E2		180 / 20	150 / 17	120 / 10	165 / 20	120 / 10	65 / 6	140 / 21
E3	165 / 12	180 / 20	150 / 17	120 / 10	165 / 20	120 / 10	65 / 6	140 / 21
E4			150 / 17	120 / 10	165 / 20	120 / 10	65 / 6	140 / 21
B1			150 / 17	120 / 10	165 / 20	120 / 10	65 / 6	140 / 21
B2			150 / 17	120 / 10	165 / 20	120 / 10	65 / 6	140 / 21
B3			150 / 17	120 / 10	165 / 20	120 / 10	65 / 6	140 / 21
B4		180 / 20	150 / 17	120 / 10	165 / 20	120 / 10	65 / 6	140 / 21

Table 3. Maximum curing conditions for the oven simulating process. Two re-runs are added for the sealer/NVH oven and primer surface oven and one re-run is added for the top coat oven to simulate the maximum curing with re-runs.

Material	Pre.cur VCBC [°C/min]	EC [°C/min]	Sealer/NVH [°C/min]	Water Drying [°C/min]	Primer Surf. [°C/min]	Water drying [°C/min]	Base coat dry. [°C/min]	Top coat [°C/min]
E1	180 / 15	200 / 30	175 / 23	140 / 13	175 / 25	140 / 13	80 / 6	155 / 24
E2		200 / 30	175 / 23	140 / 13	175 / 25	140 / 13	80 / 6	155 / 24
E3	180 / 15	200 / 30	175 / 23	140 / 13	175 / 25	140 / 13	80 / 6	155 / 24
E4			175 / 23	140 / 13	175 / 25	140 / 13	80 / 6	155 / 24
B1			175 / 23	140 / 13	175 / 25	140 / 13	80 / 6	155 / 24
B2			175 / 23	140 / 13	175 / 25	140 / 13	80 / 6	155 / 24
B3			175 / 23	140 / 13	175 / 25	140 / 13	80 / 6	155 / 24
B4		200 / 30	175 / 23	140 / 13	175 / 25	140 / 13	80 / 6	155 / 24

3.6. **Process verification**

The process simulations have been performed in laboratory ovens. In order to verify the results relative to the manufacturing process, two materials were applied on the roof of a scrap car body as shown in Figure 16. The materials used were B2 and B3. B2 and B3 were chosen since they are applied on visible areas. There were six panels of each material. The sealer oven was passed five times for the car body, after each time one panel was removed. Finally a new panel for each material was placed on the roof and the car body was run through all the ovens. Hardness and colour was measured for all panels.

Figure 16. The panels were placed on the roof of a car body for the process verification. The applied materials were B2 and B3.

3.7. DMTA

The instrument used was an Advanced Rheometer, AR 2000, from TA instruments. The measuring geometry was rectangular torsion. Before the measurements, some preparation of the equipment was necessary. The first procedure was to perform a zero gap setting and mapping the instrument. The dimension of the rod samples were measured; length, width and thickness. The sample was inserted, a torque wrench was used so the attachment was identical for each sample since this can influence the result. The sample must have smooth sides, abrasive paper was used when necessary. The thickness of the samples was dependent on the rigidity. For softer materials a thicker sample was used in order to avoid fluttering of the material and get a stable torque response in damping measurements.

For each material a strain-sweep was performed in order to identify the linear viscoelastic region. In a strain sweep test, the frequency is fixed and the strain is incrementally increased. This was carried out at three different frequencies; 0,1, 1,0 and 10 Hz.

The temperature ramp test shows shear storage modulus G', loss modulus G" and damping factor, tan δ, versus temperature. The glass transition temperature, T_g is obtained from the graph as the maximum damping temperature. The temperature was ramped, from – 90 °C to 100 °C which includes the glass transition temperature for all investigated materials. Cooling was performed using liquid nitrogen. The temperature ramping involves a continuous increased temperature per minute; in these experiments 2 °C per minute and all measurements were performed at 1 Hz. During the temperature ramp a normal force was applied to keep the material stretched, since the material changes in dimensions within the temperature range. Repeatability measurements have been performed for sample B3 and are shown in Appendix I.

Figure 17. DMTA equipment showing sample B3 attached to the clamps.

3.8. TGA

The instrument used was a Mettler Toledo TGA 850. The empty open aluminium pans were placed on the platform used for holding the pans. In the software STARe the method was outlines as shown in Appendix II. All the pans were tared. The samples were cut into small pieces about 20 mg, which give a large surface area, they were placed into the pans. One pan was kept empty and used as a reference. Nitrogen atmosphere was used up to 800 °C; the samples were then combusted in oxygen atmosphere.

3.9. DSC

The DSC measurements were performed with a Perkin Elmer DSC 7 instrument. Nitrogen flow was applied to the cooling system. The equipment was calibrated with indium. A reference sample was used to create a baseline for the background signal. This was used to correct the result from the investigated samples. Approximately 5-10 mg of the samples were cut in pieces and placed in crucibles with perforated lids to obtain a total inert atmosphere with nitrogen. The crucibles and lids were folded by compression. The temperature was ramped with a temperature increase of 5 °C/min or 20°C/min, from – 30 to 240 °C, which is the interval where T_g is expected. The experimental conditions are presented in Appendix III.

In order to further investigate the ability to use DSC as quality control of the materials during the manufacturing process a more advanced DSC equipment was used. Els Verdonck at TA instrument gave Volvo Cars and this master thesis the possibility to investigate the ability of finding T_g in their Q2000 DSC equipment. Els helped with her experience in using DSC equipment. The temperature and enthalpy calibration was performed with indium. 20-30 mg of the samples was placed in Tzero hermetic aluminum cups. The heating rate was 20 °C/min and the nitrogen purge was 50 ml/min. The temperature was raised from -80 to 40 °C. Three samples were sent to TA instruments, NC, MC and MCR for E2.

3.10. FTIR

The FTIR used was a Perkin Elmer BXII, ATR-FTIR with a zinc selenide crystal. The obtained spectra were normalized in order to compare the peaks.

3.11. Colour testing (colourimetry)

To perform the colour measurements a MA68II Multi-angle spectrophotometer X-rite was used. Firstly, a calibration was performed where the spectrophotometer was applied to a totally reflecting white box and to a totally absorbing black box. The computer software ProQnet.vi was used. First a reference sample, NC, was scanned and used as a master, then the two comparing samples, MC and MCR, were scanned. The resulting colour opponent dimensions were derivate colour differences from the master sample. The colour was measured at five different angles. The total colour difference dE relative to NC is calculated for each angle, 15 °, 25 °, 45 °, 75 ° and 110 °, and the average value was calculated.

3.12. Hardness testing

The instrument used for the softer materials was International Gummi–Härtegrade IRH-micro DIN 53519-2 micro, manufactured by BAREISS and Shore D DIN 53505, Zwick. The sample was placed on the instrument. The measuring cantilever was adjusted to the surface of the sample. The cantilever was penetrating the sample for 30 seconds, at a given load then the hardness value was shown on the display. For each material the measurements were repeated five times and the average hardness was calculated. For the harder materials a Shore D durometer was used with a sharp cone penetrated the sample. This method was using a mechanical load were the arm was pulled with a constant force and the result was noted immediately.

3.13. **Swelling**

The polybutadiene-based materials were exposed to different solvents in order to evaluate the visible interactions between the polybutadiene and the solvent. Thin rods of the polymer were immersed in toluene, tetrahydrofuran, dimethyl chloride and butyl acetate for five hours. The measure of swelling was given as the change in length. Toluene gave the best result and was also used in literature, thus toluene was used in this study.

Rods with approximately the same dimensions were prepared. The length of all the samples was measured using a magnifying glass before swelling. The rods were placed in small glass jars, 8 ml toluene was added. The rods were totally covered with toluene. The length was measured after every hour to assess when steady state was reached. After five hours there was no further increase in length and steady state was assumed.

4. Results

In this section the experimental results are presented. The section is divided into three parts; polybutadiene, epoxy and PVC-based material. The DMTA, TGA and DSC results are illustrated in graphs. Glass transition temperatures, hardness and colour changes are presented in tables. The obtained FTIR results are commented on. The results from the process verification are shown. For complete results, see Appendix I - VII.

4.1. Polybutadiene-based materials E1, E2 and E3

4.1.1. DMTA

The glass transition temperature exhibited a negligible shift for E1 at all curing conditions. There was a small change in damping factor for the three experiments. MC gave the highest damping factor, MCR had a lower damping factor and NC the lowest, illustrated in Figure 18 and Table 4. At 25 °C, the loss modulus G", indicates a somewhat softer material for the NC sample, since the viscous response is higher. The damping factor tan (δ) displayed one clear peak, possible also affected by shoulders connected to other transition than T_g.

T_g for E2 was shifted towards higher temperatures for MC and MCR. The damping factor was higher for MC and MCR. There were probably two peaks in damping curve for the NC sample. There was no indication of changes in crosslinking density in the graph, since the storage modulus was equal at higher temperatures for these damping cases illustrated in Figure 19 and Table 4. At low temperatures, NC and MC specimens exhibited a higher G' – value than the MCR sample.

For E3, there were a significant difference in T_g and damping factor between NC and the other two specimens. The first peak (lowest in temperature) is probably associated with the polybutadiene-phase of the material and is shifted towards higher temperatures with MC and MCR, when compared with NC, shown in Figure 20. At second peak in the tan (δ)-curve was also evident and this peak did not change markedly in position for the three different cases. For this material it was observed that the highest crosslink density, i.e. the highest storage modulus at higher temperatures, was obtained for the sample with MCR, shown in Figure 20 and Table 4. The flattening of the storage modulus curve G', between the temperatures 50 °C to 100 °C indicates an increased crosslink density. The NC and MC conditions showed a lower crosslink density. The two peaks for tan (δ) in the DMTA curve can probably be explained by an existence of two different polymers in the material.

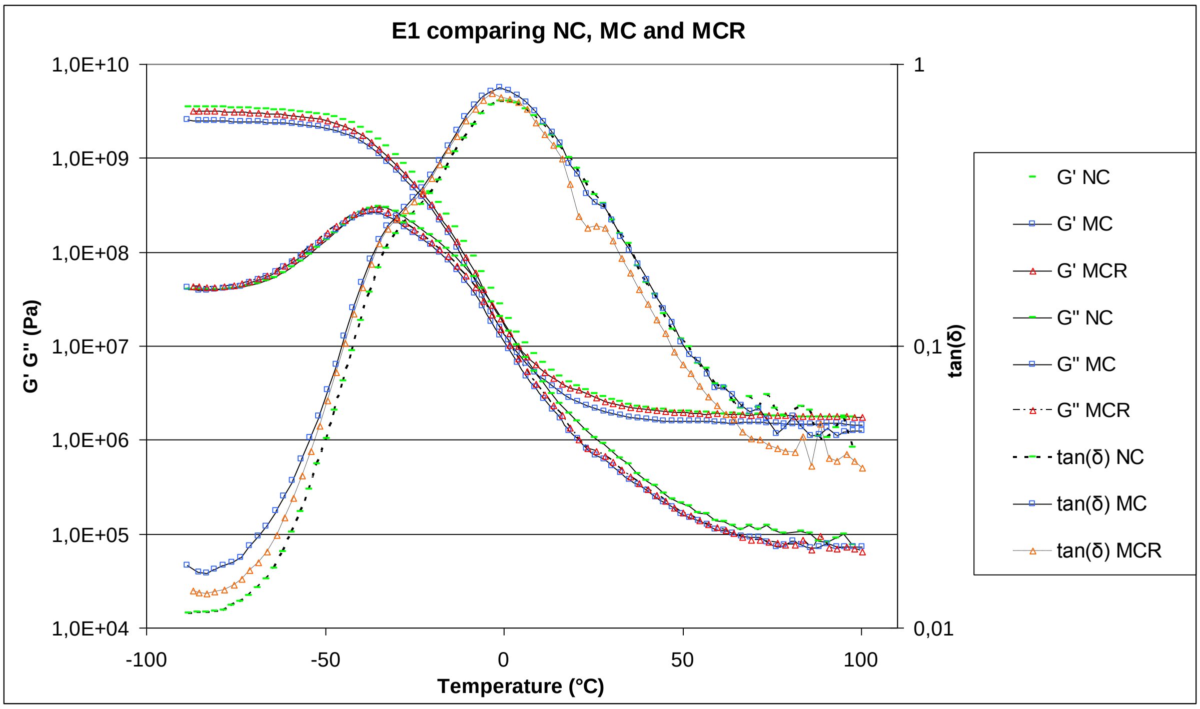

Figure 18. DMTA results for E1. The curves that corresponds to the experiments are NC (green lines), MC (blue squares) and MCR (red triangles). The experimental conditions were 0,01 % strain, the torque for the sample attachment 9 N/m and frequency 1Hz.

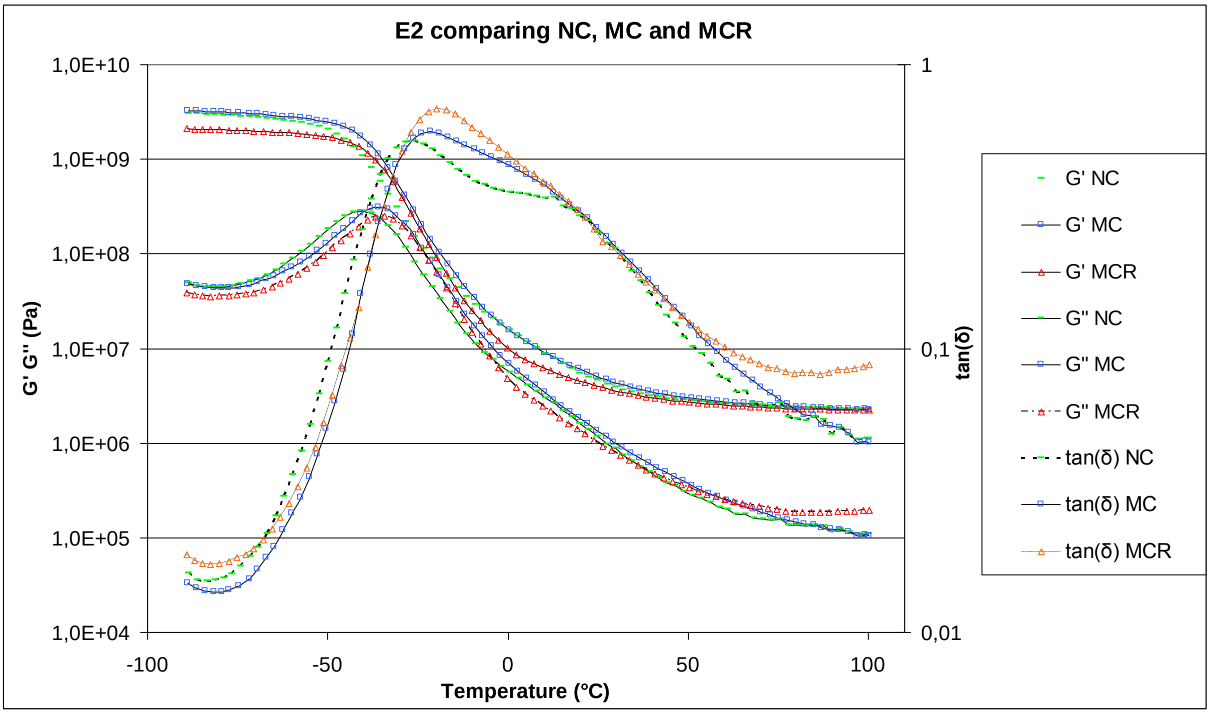

Figure 19. DMTA results for E2. The curves that corresponds to the experiments are NC (green lines), MC (blue squares) and MCR (red triangles). The experimental conditions were 0,02 % strain, the torque for the sample attachment 9 N/m and frequency 1Hz.

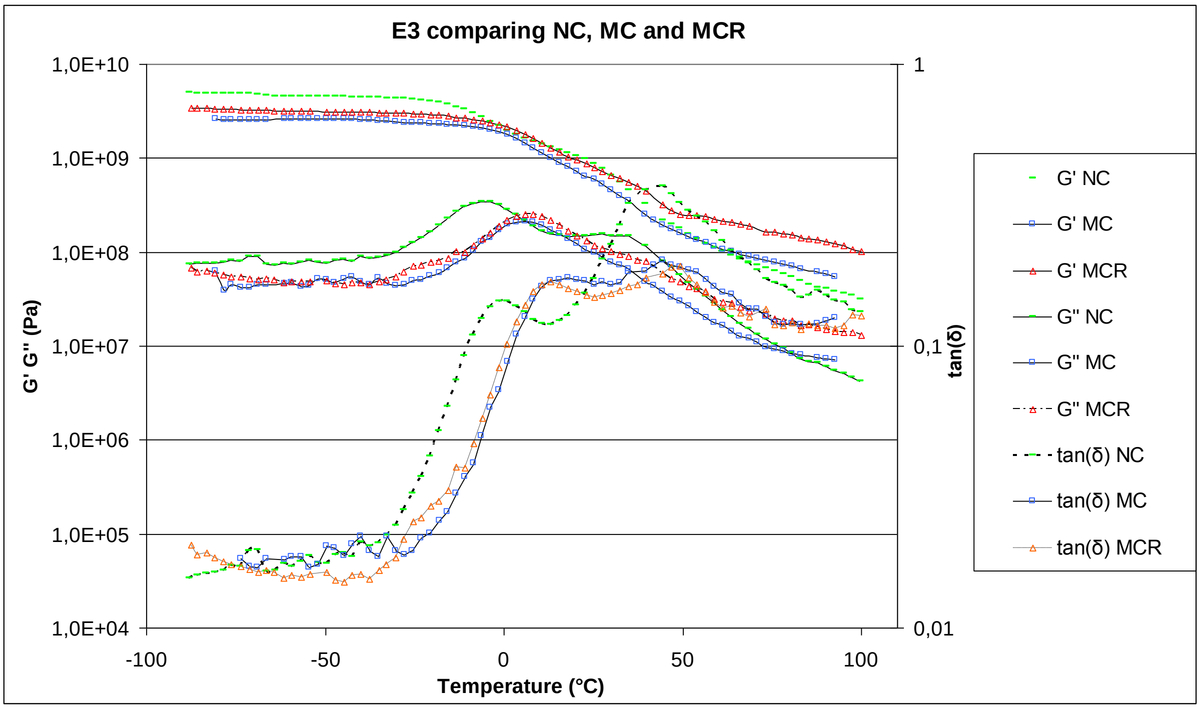

Figure 20. DMTA results for E3. The curves that corresponds to the experiments are NC (green lines), MC (blue squares) and MCR (red triangles). The experimental conditions were 0,01 % strain, the torque for the sample attachment 9 N/m and frequency 1Hz.

Table 4. The glass transition temperatures and the maximum damping factor for E1, E2 and E3. For E3 two peaks were noted, data from each peak is presented in the table. First column represent the first peak for T_g and tan (δ).

<table>
<tr><th>Material</th><th colspan="4">Normal curing</th><th colspan="4">Maximum curing</th><th colspan="4">Maximum curing with re-runs</th></tr>
<tr><td></td><td colspan="2">T_g [˚C]</td><td colspan="2">tan(δ)</td><td colspan="2">T_g [˚C]</td><td colspan="2">tan(δ)</td><td colspan="2">T_g [˚C]</td><td colspan="2">tan(δ)</td></tr>
<tr><td>E1</td><td colspan="2">-1,2</td><td colspan="2">0,74</td><td colspan="2">-1,0</td><td colspan="2">0,82</td><td colspan="2">-3,2</td><td colspan="2">0,79</td></tr>
<tr><td>E2</td><td colspan="2">-25,9</td><td colspan="2">0,54</td><td colspan="2">-21,4</td><td colspan="2">0,58</td><td colspan="2">-19,8</td><td colspan="2">0,70</td></tr>
<tr><td>E3</td><td>2,1</td><td>44,3</td><td>0,11</td><td>0,37</td><td>15,6</td><td>44,3</td><td>0,17</td><td>0,41</td><td>13,1</td><td>49,2</td><td>0,17</td><td>0,22</td></tr>
</table>

4.1.2. TGA

The results showed that the different curing conditions had no effect on the subsequent thermal degradation. The first decrease in the curve represents the loss of plasticizer and unreacted vulcanization agents, the next mass loss is caused by degradation and finally the polymeric material becomes decomposed, for example shown in Figure 21. Approximately at 200 °C the solvent and unreacted species were released. Degradation started around 350 °C when all the thermal stabilizers were consumed. From 500 °C decomposition was observed. The ash content refers to the remaining inorganic substances, i.e. the fillers. For E1 the ash content was 30,8 %, E2 had 37,7 % and 49,4 % for E3.

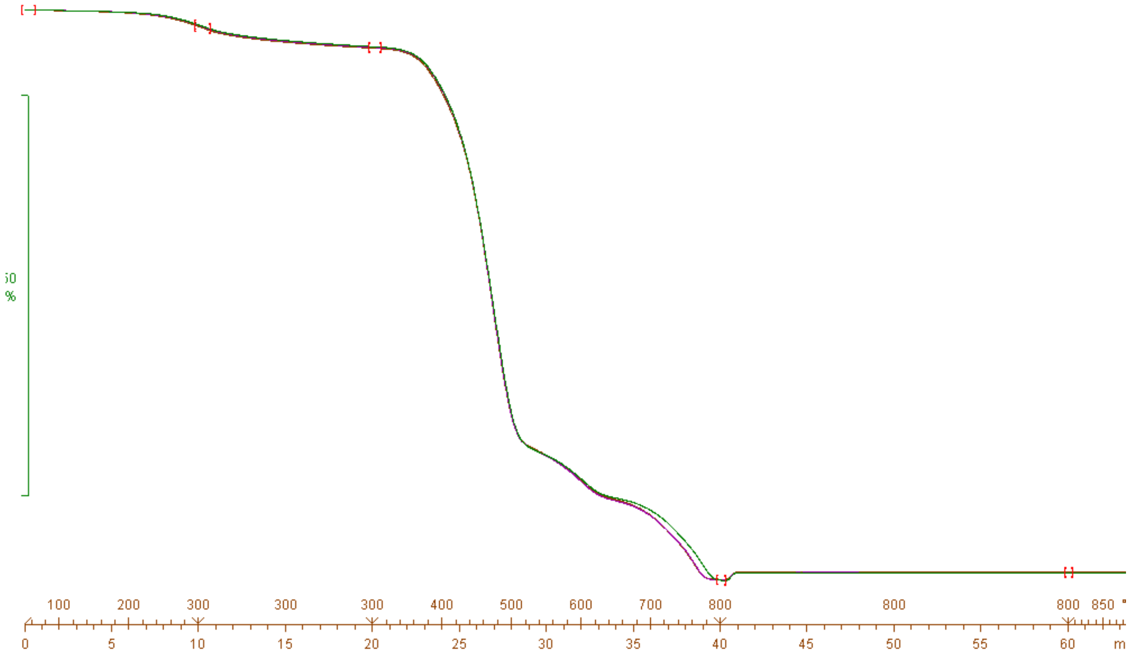

Figure 21. TGA results for E1. The remaining ash content was 30, 8 % after the oxygen combusting. NC (turquoise), MC (blue) and MCR (black) are shown.

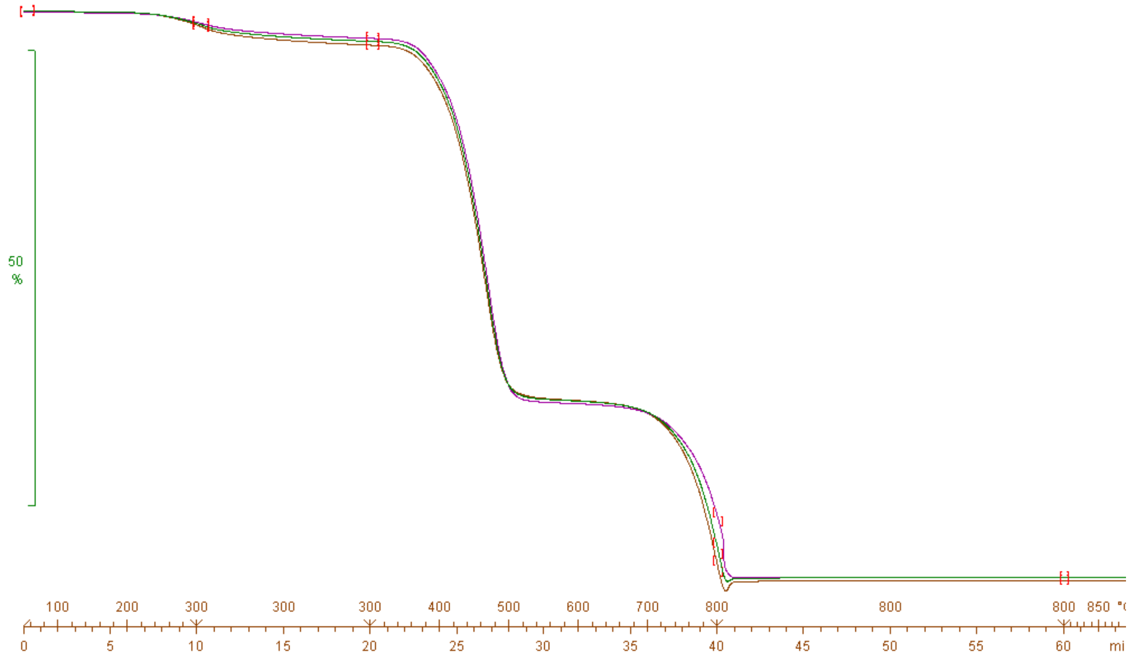

Figure 22. Result from TGA for E2. 37,7 % was the remaining ash content for E2. NC (green), MC (blue) and MCR (pink) are shown.

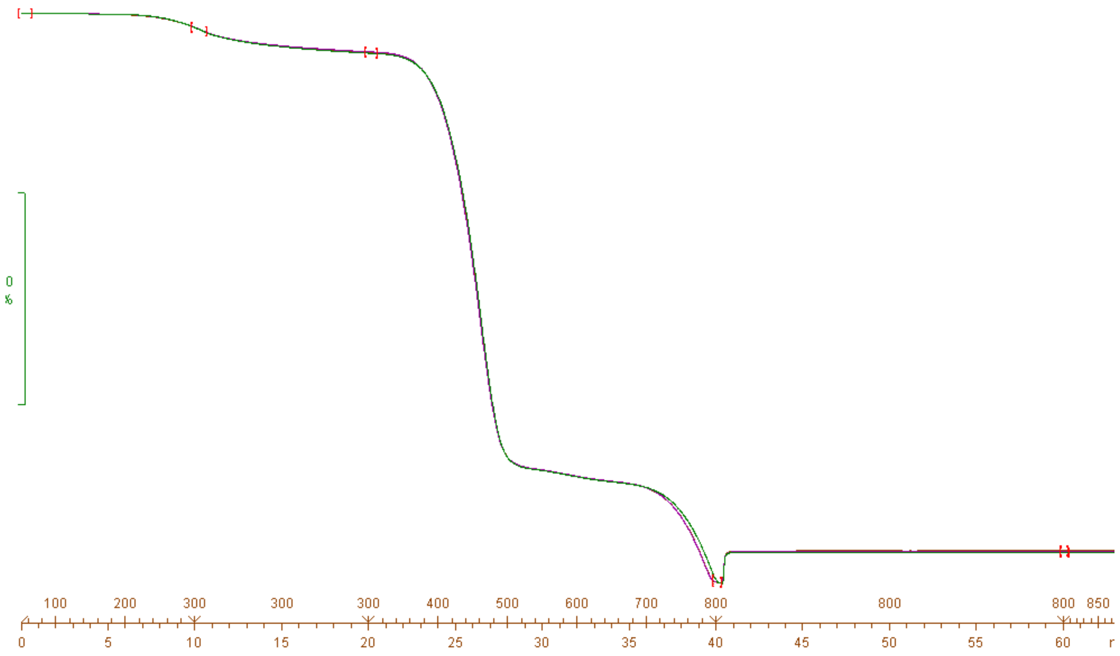

Figure 23. TGA results for E3. The ash content after total combustion with oxygen was 49,4 %. NC (turquoise), MC (blue) and MCR (purple) are shown.

4.1.3. **DSC**

The intention was to use DSC as a quick and precise method to measure T_g. The complication in finding T_g in all material by using Perkin Elmer DSC 7 instrument was observed during the experiments. The equipment was not that sensitive and advanced as it needs to be when investigating thermoset materials. Therefore, no information could be used from the measurements. This is illustrated in Figure 24. This phenomenon was also noted for the remaining investigated materials, and those graphs are only showed in Appendix III.

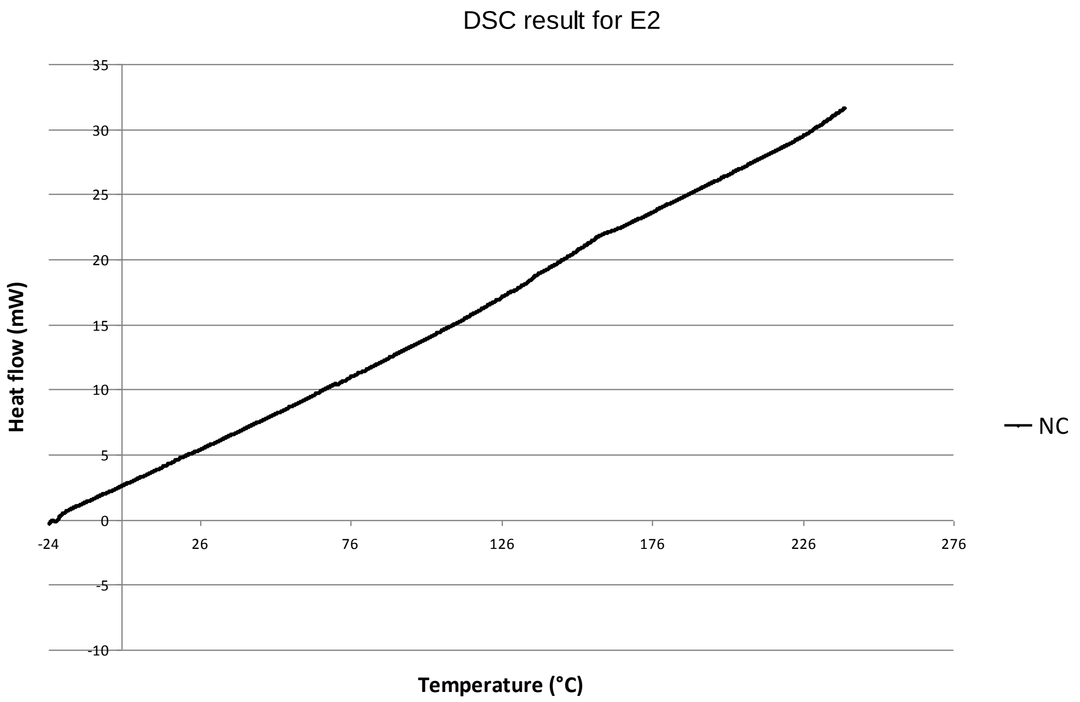

Figure 24. DSC result for the NC sample, E2. Temperature ramp from -30 to 240 °C.

Figure 25 illustrates the result for E2 (NC, MC and MCR) from the DCS measurement that TA instruments and Els Verdonck made with a more advanced equipment. NC has a T_g at -38,6 ° C, MC has a shift in T_g to -33,5 °C and MCR has also a shifted T_g at -30,57 °C. The calculations of T_g for the three experiments are shown in Appendix III.

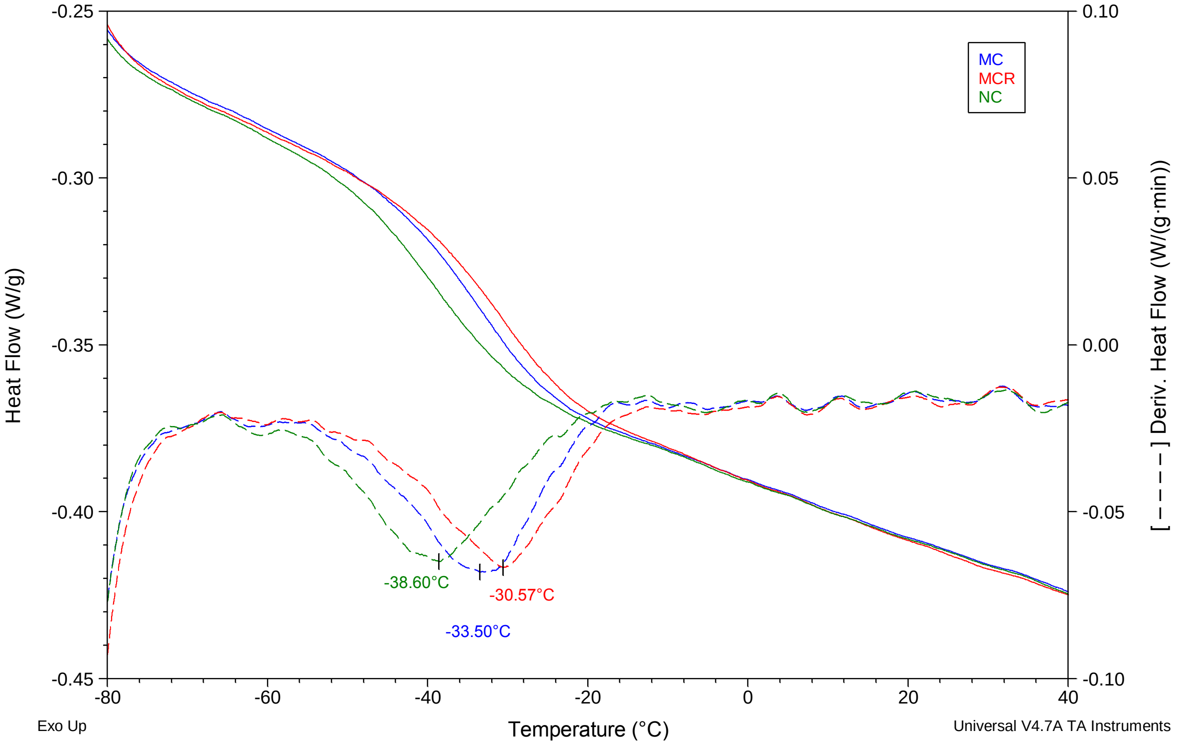

Figure 25. DSC result for E2 measured by Els Verdonck on TA instruments. Temperature ramp from -80 to 40 °C showing NC (green), MC (blue) and MCR (red)

4.1.4. FTIR

FTIR was used to investigate the curing development in the polybutadiene-based materials. During curing sulfur reacts with the alternating double bonds in the polymeric chain. E1 and E2 had a difference in absorption between the NC material and the MC at the C-H peaks around 2900 cm^{-1}. For E2 and E3 there were an increase in amine bonds which corresponds to a broad peak at approximately 3200 cm^{-1} shown in Figure 27 and Figure 28. The NC E1 sample has a sp^2 carbon absorption at 3071 cm^{-1} which decreased for MC and MCR, see Figure 26. This phenomenon was also observed for E2 and E3. The decrease in absorption around 3000 cm^{-1} can be explained by increased crosslinking, since carbon double bonds are consumed.

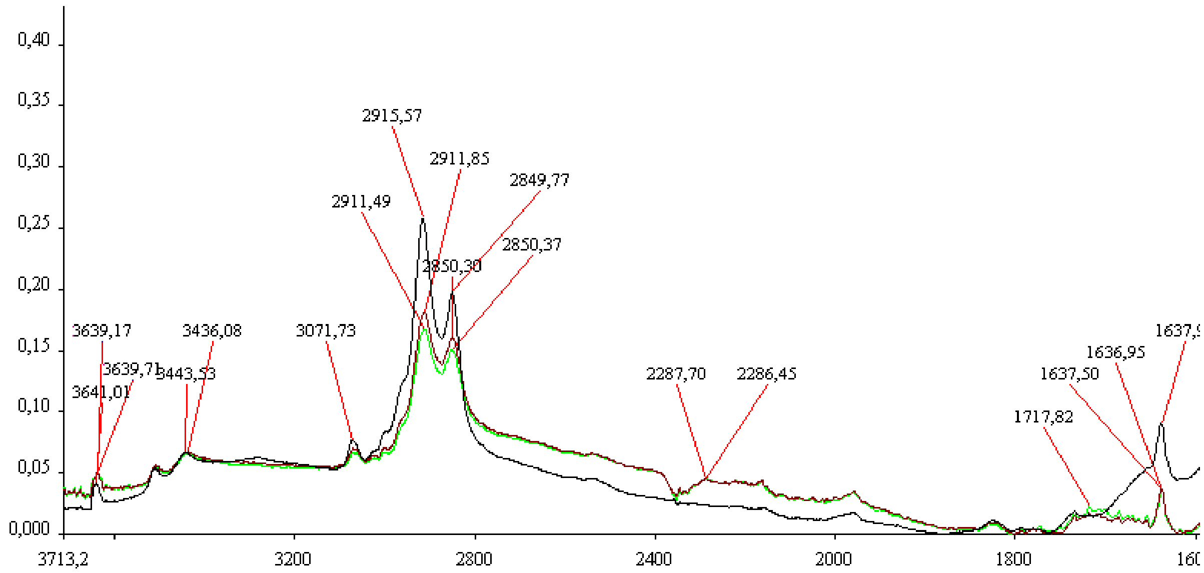

Figure 26. Normalized graph of E1, for the NC (black line). There is a peak at 3071 for a carbon double bond. MC (brown line) and MCR (green line) resembles to each other. Energy monitored 1240 >1050 J.

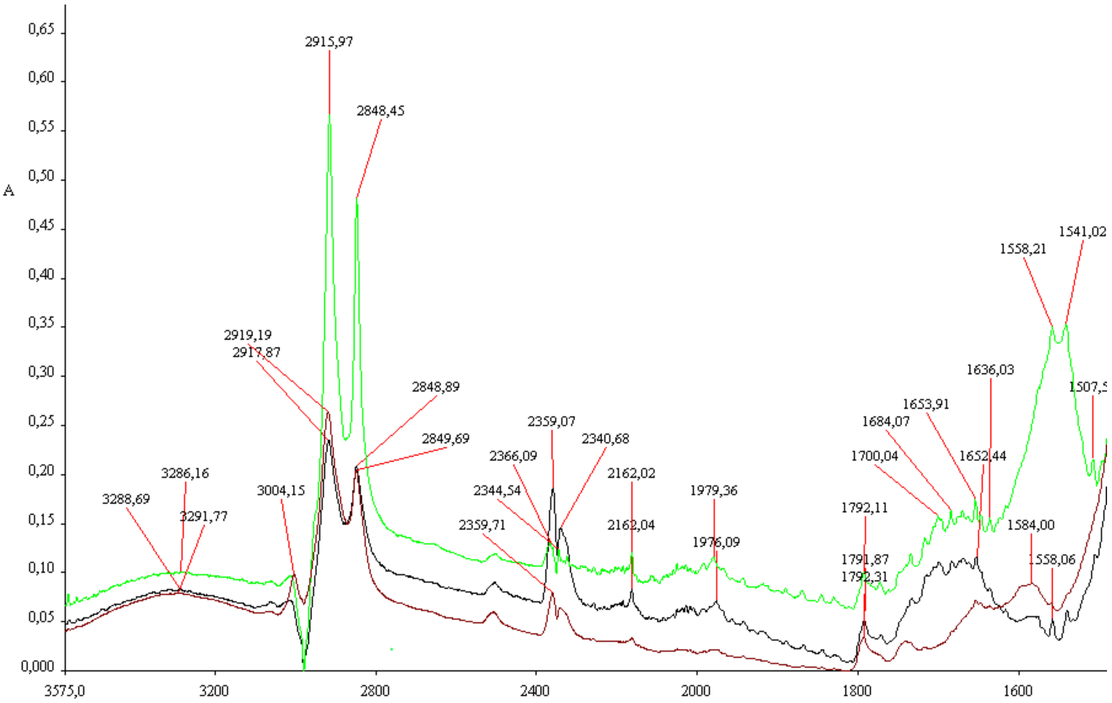

Figure 27. Normalized graph of E2 showing a carbon double bond for the NC sample at 3004 cm^{-1} (brown line), MC (black) and the MCR (green line). The C-H bond at 2916 cm^{-1} is much stronger. Energy monitored 1247>1150 J.

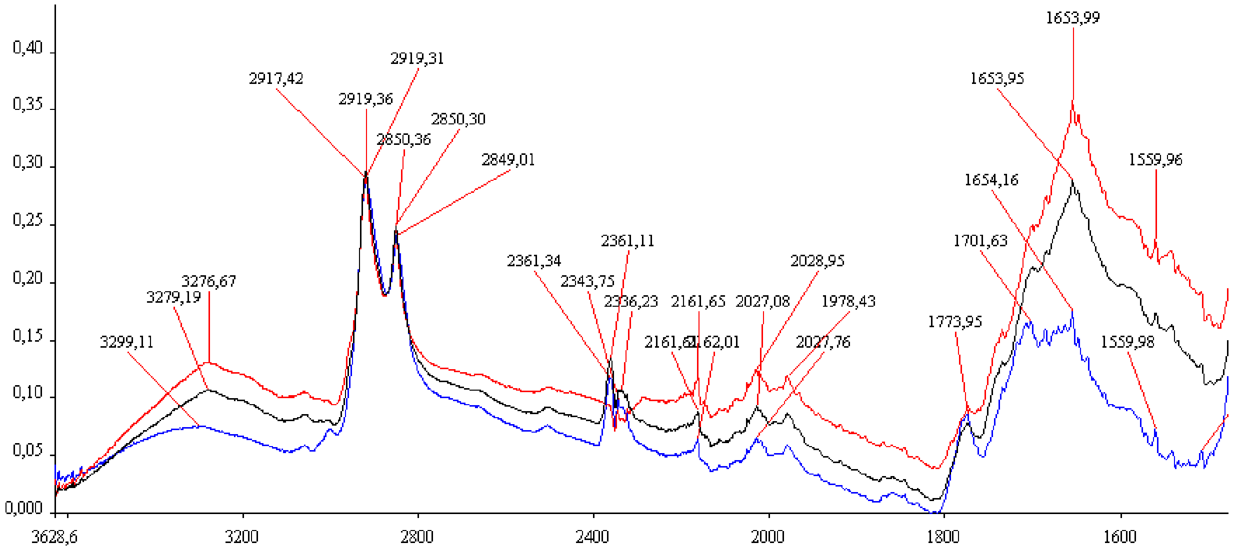

Figure 28. Normalized graph of E3. NC (blue line) has a small peak at 3001 cm^{-1}. MC (black line) and MCR (red line). Energy monitored 1242 >1057 J.

4.1.5. Colour testing

The polybutadiene-based materials are applied on hidden parts on the car body. Therefore it is not possible to measure the colour during the car manufacturing. The colour on the surface was deviating due to oxidative reactions in the simulation process causing an inaccuracy of measuring values. The results are presented in Appendix V.

4.1.6. Hardness testing

For E1 there was a significant increase in hardness between NC and MC, shown in Table 5. In case of E2 the hardness increased considerably for each step. This was also the case for E3, but not as pronounced as for E2.

Table 5. Hardness test results for E1, E2 and E3

Experiment	**E1 IRHD-micro**	**E2 IRHD-micro**	**E3 Shore D**
Normal curing	42,3	50,3	61,8
Maximum curing	49,0	60,3	66,2
Maximum curing with re-runs	49,8	77,2	68,2

4.1.7. Swelling testing

The trend for E1, E2 and E3 was a decreased swelling with increasing curing times and temperatures as shown in Table 6. E3 showed no notable difference between MC and MCR, NC swelled significantly more than the others.

Table 6. Results from swelling test for E1, E2 and E3. The length was measured after 5 hours and compared to the original length. The solvent used was toluene at 25 °C.

	Percentage increased length [%]		
	E1	E2	E3
Normal curing	28,8	36,0	14,8
Maximum curing	25,6	32,2	8,1
Maximum curing with re-runs	21,6	26,2	7,6

4.2. **Epoxy-based material, E4**

4.2.1. **DMTA**

The T_g was shifted to higher temperatures with the two MC conditions. The tendency observed was a reduction of the damping factor for the MC and MCR. This was especially pronounces in the case of MCR, see Figure 29 and Table 7. The storage modulus curve for MCR was more flat than for NC and MC indicating a more crosslinked material and, at higher temperatures, the G' for MCR was also increased compared to the other curing schemes.

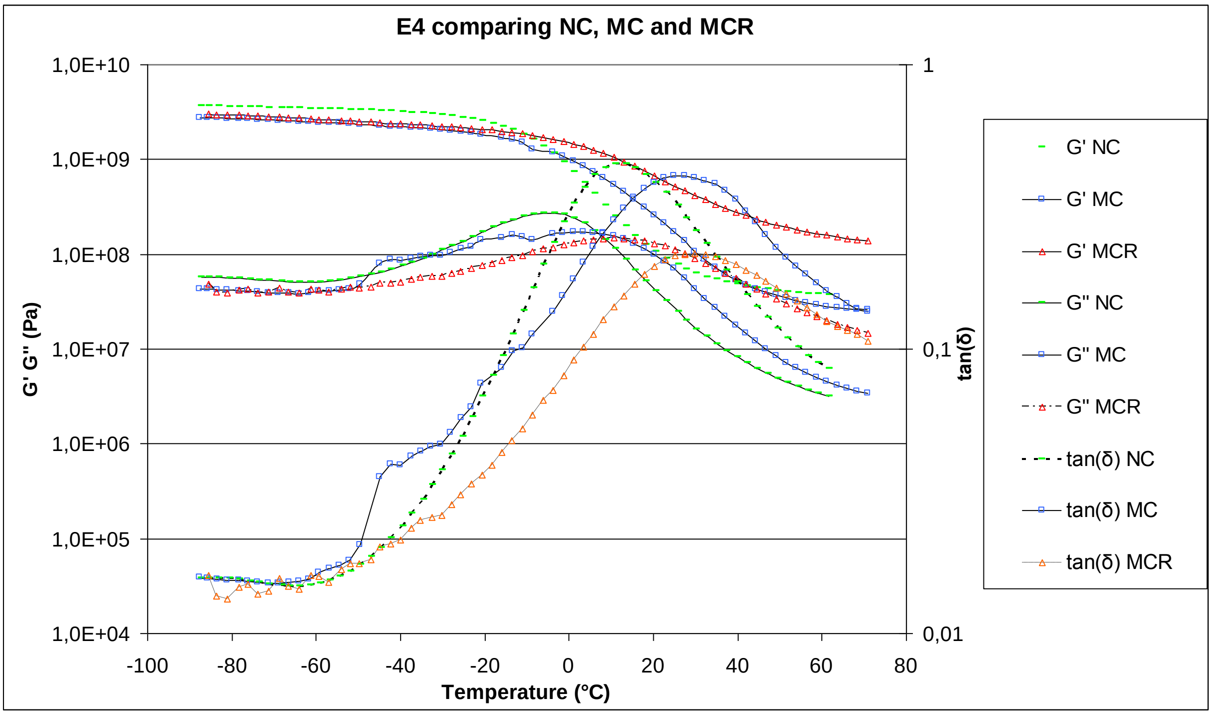

Figure 29. DMTA results for E4. The curves that corresponds to the experiments are NC (green lines), MC (blue squares) and MCR (red triangles). The experimental conditions were 0,015 % strain, the torque for the sample attachment was 28 N/m and the frequency 1Hz.

Table 7. The glass transition temperatures and the maximum damping factor for E4

Material	**Normal curing**		**Maximum curing**		**Maximum curing with re-runs**	
	T_g [˚C]	tan(δ)	T_g [˚C]	tan(δ)	T_g [˚C]	tan(δ)
E4	11,1	0,45	27,4	0,41	29,9	0,22

4.2.2. **TGA**

The mass loss curves are shown in Figure 30. First mass loss, at 300 °C, is a result of dehydration due to elimination of water from the propylene group leading to subsequent formation of double bonds. The scission of the polymeric chain yielded unsaturated phenolic compounds which produced a char, at 350 °C. The mass loss curve was quite similar for all curing conditions.

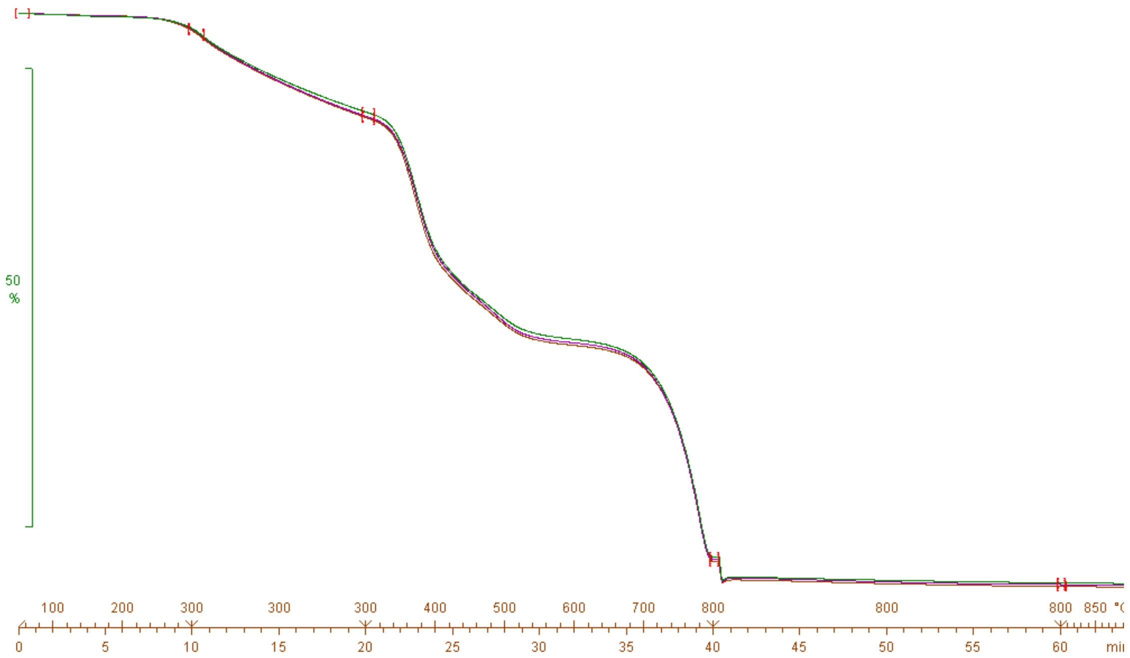

Figure 30. TGA result for E4. The ash content after combustion in oxygen was 38,1 %. NC (purple), MC (blue) and MCR (black) are presented.

4.2.3. **Colour testing**

The colour shifted to a darker colour for the MC sample. After the additional curing procedure, MCR, the colour became darker, as shown Table 8.

Table 8. Results from colour testing, NC was the reference sample

Sample	**Total colour difference (dE) from averaging of the five measurement angles, 15 – 110 °**
E4 MC	6,7
E4 MCR	22,7

4.2.4. **Hardness testing**

The hardness was increased for all curing conditions, as shown in Table 9.

Table 9. Hardness results for E4

Experiment	**E4 Shore D**
Normal curing	60
Maximum curing	68,4
Maximum curing with re-runs	75

4.3. **PVC-based materials, B1, B2, B3 and B4**

4.3.1. **DMTA**

There was a small shift in T_g towards a higher temperature for B1, see Figure 31 and Table 10. The damping factor was somewhat higher as the curing was intensified. The storage modulus was higher for MC and MCR than for NC in the high temperature region.

For B2 T_g was shifted to significantly higher temperatures from NC to MCR. There was a trend for a decreased damping factor for the MC and MCR samples but the peak was very broad. MCR had the highest storage modulus at room temperature and above, illustrated in Figure 32 and Table 10.

B3 exhibited only minor differences between the different curing conditions with regard to T_g. In the MCR graph the storage modulus had a deviating behavior and was higher at 25°C and above, shown in Figure 33 and Table 10.

The T_g for B4 increased with longer curing times and higher temperatures, see Figure 34 and Table 10. There was a trend for decreased damping factor from NC to MCR. At 25°C, MCR had the highest storage modulus.

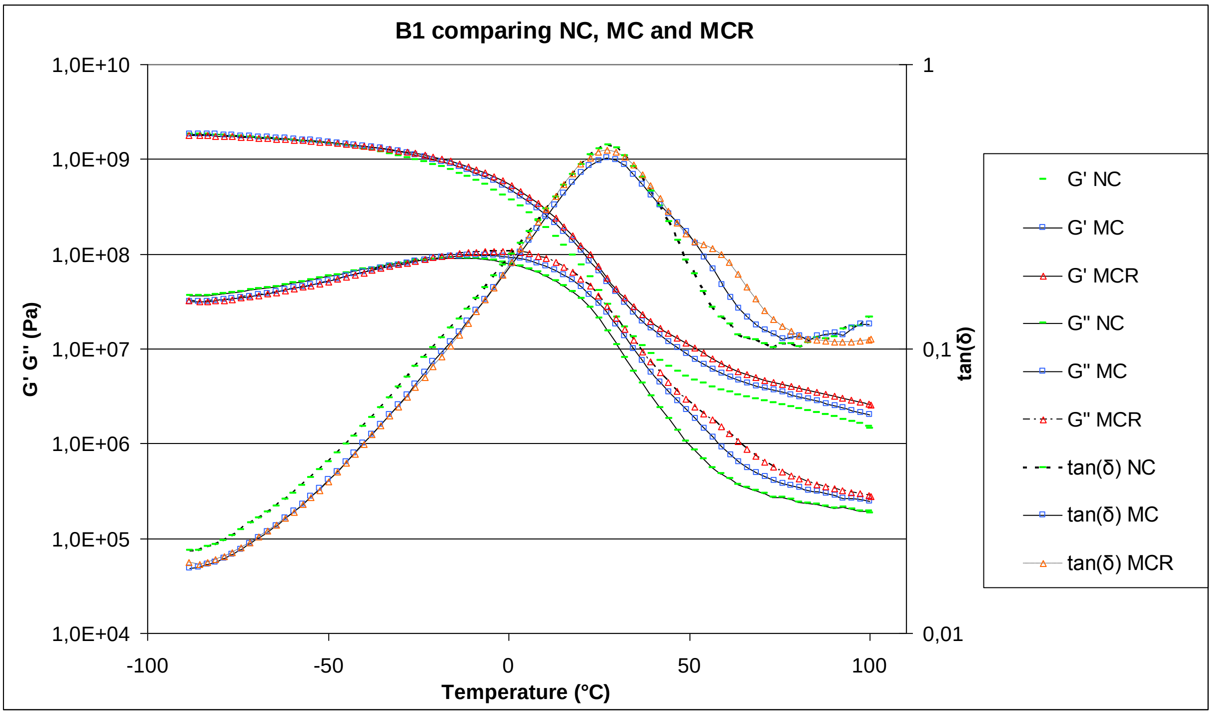

Figure 31. DMTA results for B1. The curves that corresponds to the experiments are NC (green lines), MC (blue squares) and MCR (red triangles). The experimental conditions were 0,1 % strain, the torque for the sample attachment 9 N/m and frequency 1 Hz.

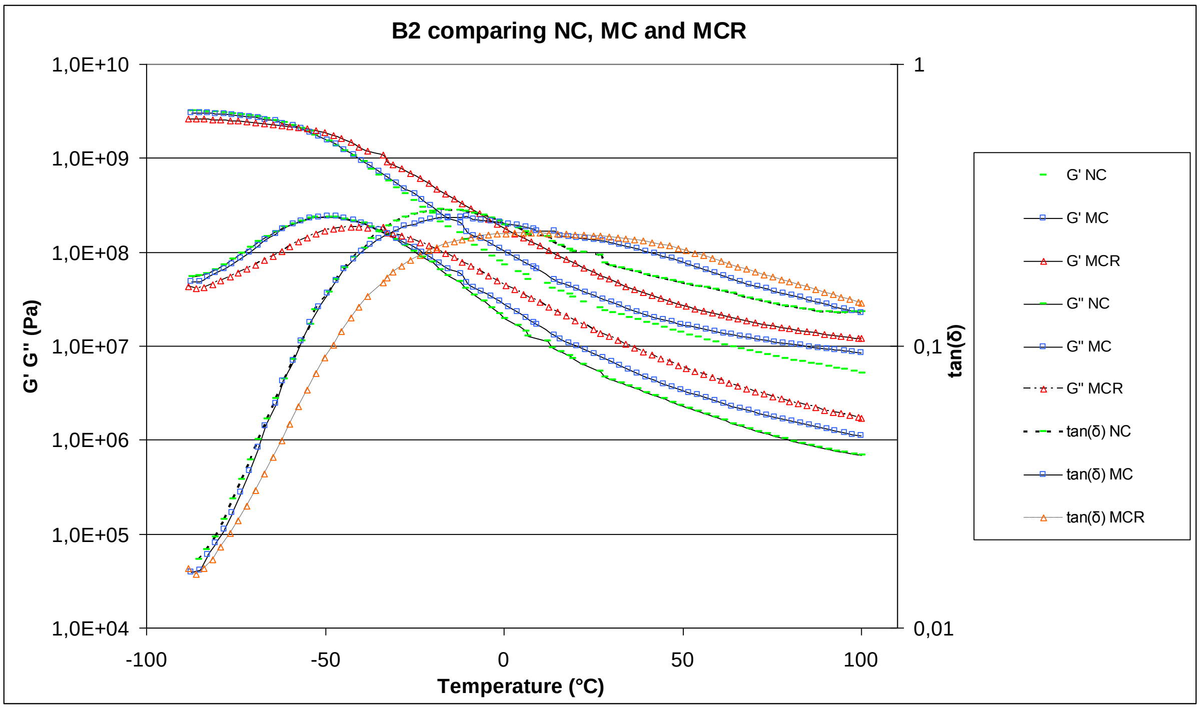

Figure 32. DMTA results for B2. The curves that corresponds to the experiments are NC (green lines), MC (blue squares) and MCR (red triangles). The experimental conditions were 0,02 % strain, the torque for the sample attachment 8 N/m and frequency 1 Hz.

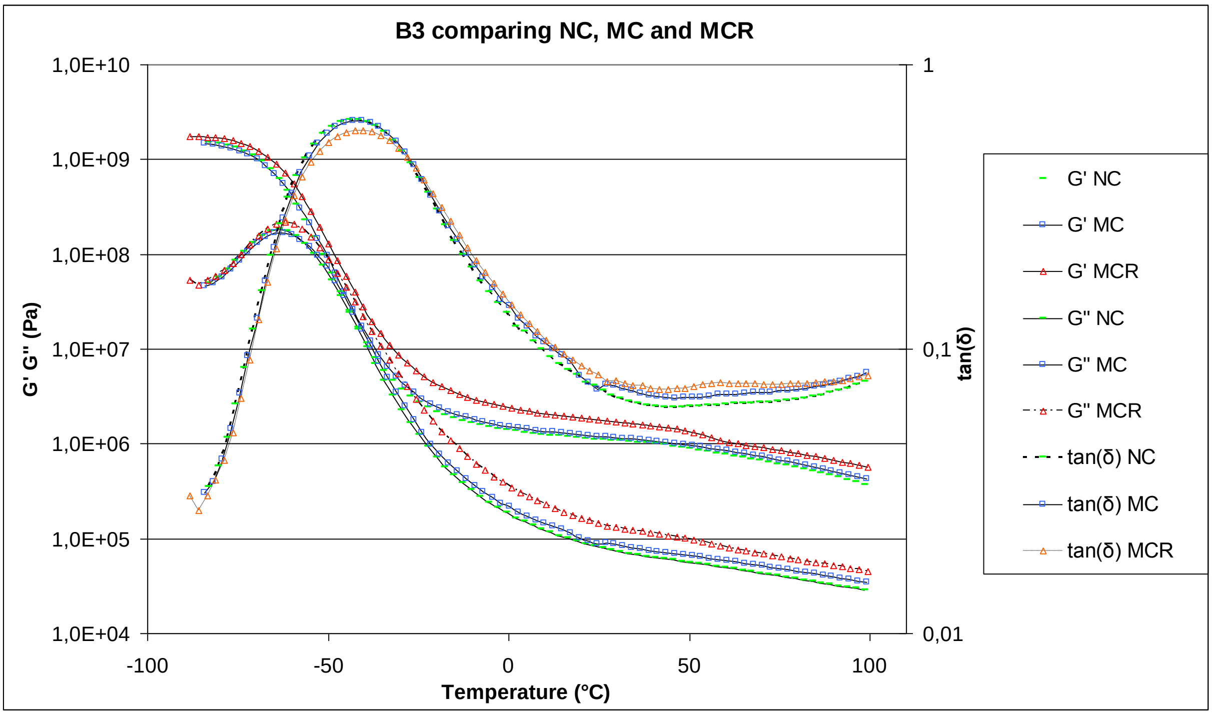

Figure 33. DMTA results for B3. The curves that corresponds to the experiments are NC (green lines), MC (blue squares) and MCR (red triangles). The experimental conditions were 0,1 % strain, the torque for the sample attachment was 8 N/m and frequency 1 Hz.

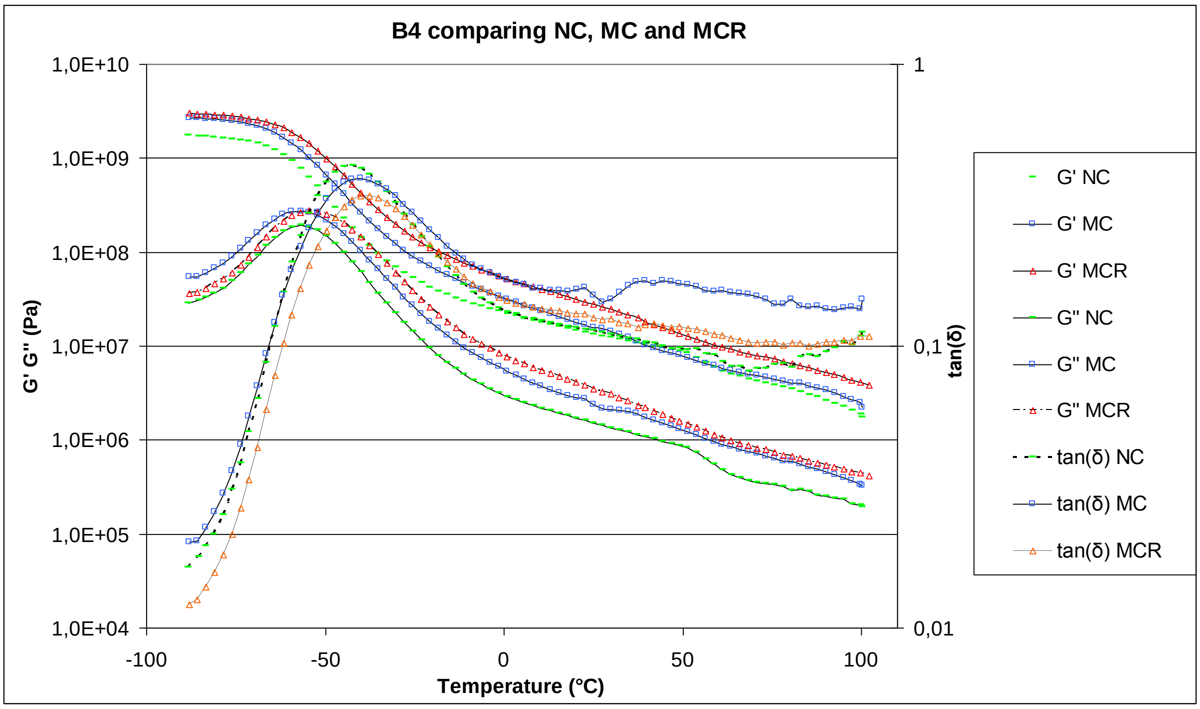

Figure 34. DMTA results for B4. The curves that corresponds to the experiments are NC (green lines), MC (blue squares) and MCR (red triangles). The experimental conditions were 0,01 % strain, the torque for the sample attachment was 28 N/m and frequency 1 Hz.

Table 10. The glass transition temperatures and the maximum damping factor for B1, B2, B3 and B4

Material	**Normal curing**		**Maximum curing**		**Maximum curing with re-runs**	
	T_g [˚C]	**tan(δ)**	**T_g [˚C]**	**tan(δ)**	**T_g [˚C]**	**tan(δ)**
B1	26,1	0,47	28,3	0,41	27,3	0,43
B2	-17,8	0,31	-10,3	0,29	0,5	0,26
B3	-41,8	0,95	-43,0	0,93	-40,4	0,82
B4	-42,3	0,43	-40,0	0,39	-37,6	0,34

4.3.2. **TGA**

For the PVC-materials the first degradation step represented the loss of volatile compounds (plasticizer and solvent). Next step refered to a loss of hydrochloric acid and during further degradation chain scission occurred. For B1 in Figure 35 the degradation started at 300 °C. The mass loss during the first step was larger for NC and MC than for MCR. The somewhat started at the same temperature for all the curing conditions. The percental ash content was higher for the sample with re-runs.

B2 had a varied amount of outgoing volatile compounds between the samples. The trend was that the sample with longer oven times and higher temperatures exhibited a lower release of volatile compounds. The percental ash content was somewhat higher for MC and MCR as shown in Figure 36.

There was a large amount of plasticizer released in the first step for B3 as shown in Figure 37. The MC and MCR were quite similar in this respect and had a smaller mass loss than the NC. The percental ash content was somewhat lower for NC than the other experiments.

The degradation steps for B4 were equal with regard to the percent mass loss. The tendency was that the amount of volatile groups was decreasing with increasing curing times as shown in Figure 38.

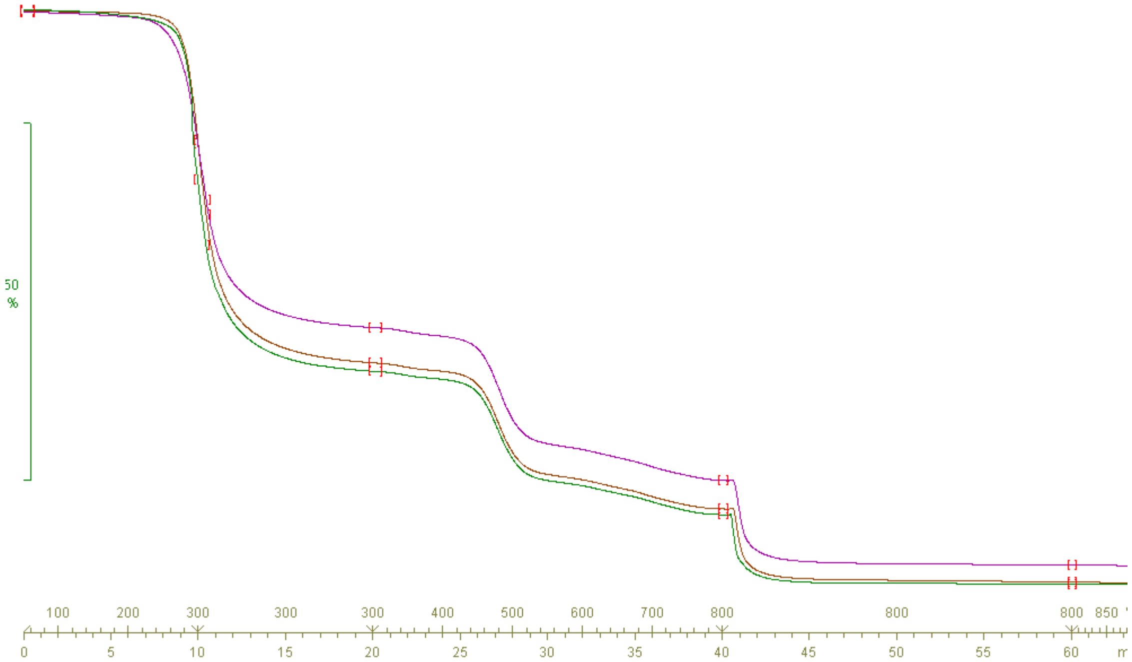

Figure 35. TGA result for B1. The ash content for NC (green) and MC (brown) was 20,1 % and MCR (purple) had 22,5 %

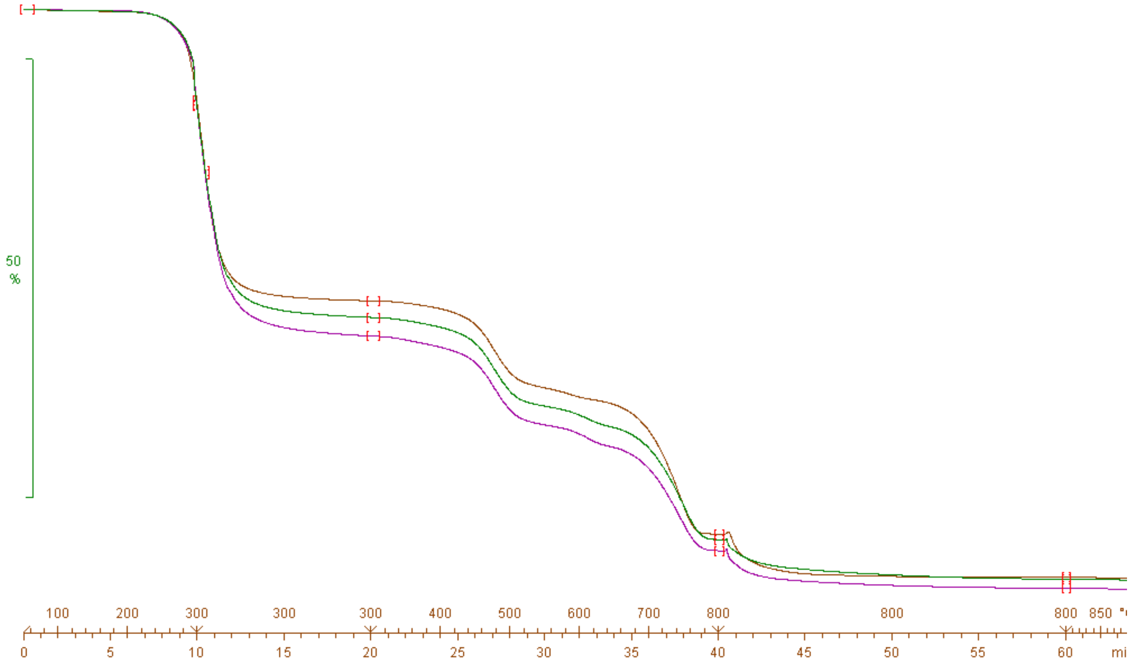

Figure 36. TGA result for B2. The ash content for NC (pink) was 34,1 % and for MC (green) and MCR (brown) were 35,3 %

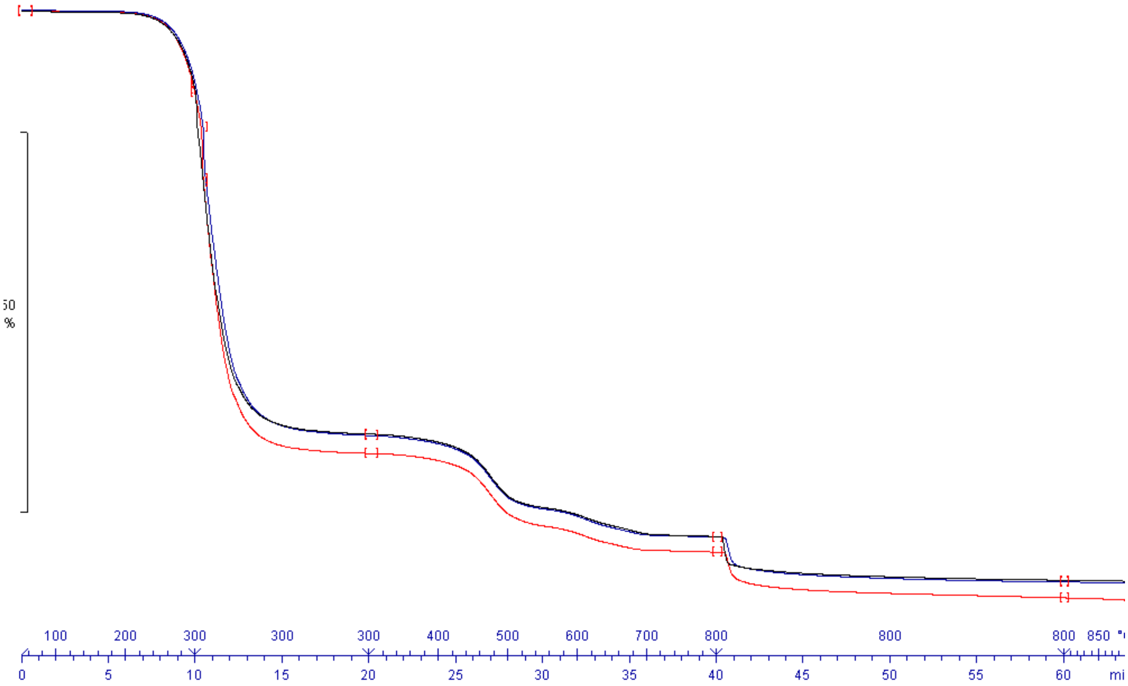

Figure 37. B3 result from TGA. Ash content for NC (red) was 23,1 % and for MC(blue) and MCR (green) 25 %

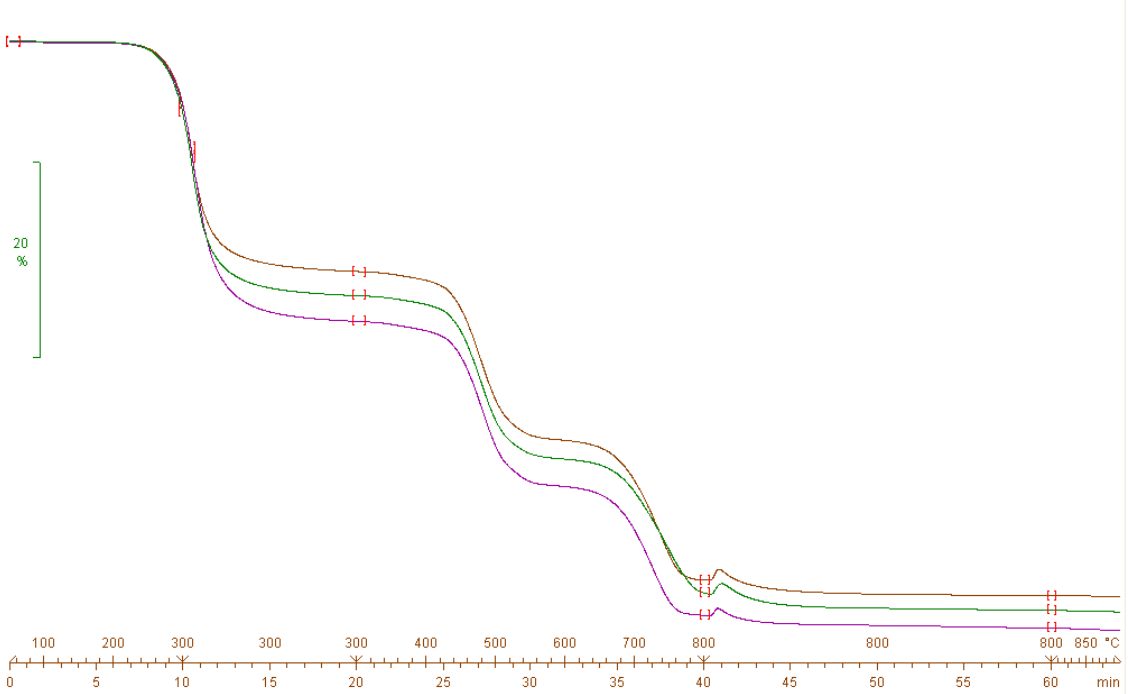

Figure 38. The TGA result for B4. Ash content for NC (purple) was 40,3 %, for MC (green) 42 % and for MCR (brown) 43,5 %

4.3.3. **FTIR**

The broad peak at 3291 cm^{-1} in the spectra for MCR, B1, indicated amine groups as illustrated in Figure 39. The absorption corresponding to the C-H peaks around 2900 cm^{-1} had increased for MCR. The FTIR results for B2, B3 and B4 showed no difference in absorption between the different curing conditions. They are attached in Appendix IV.

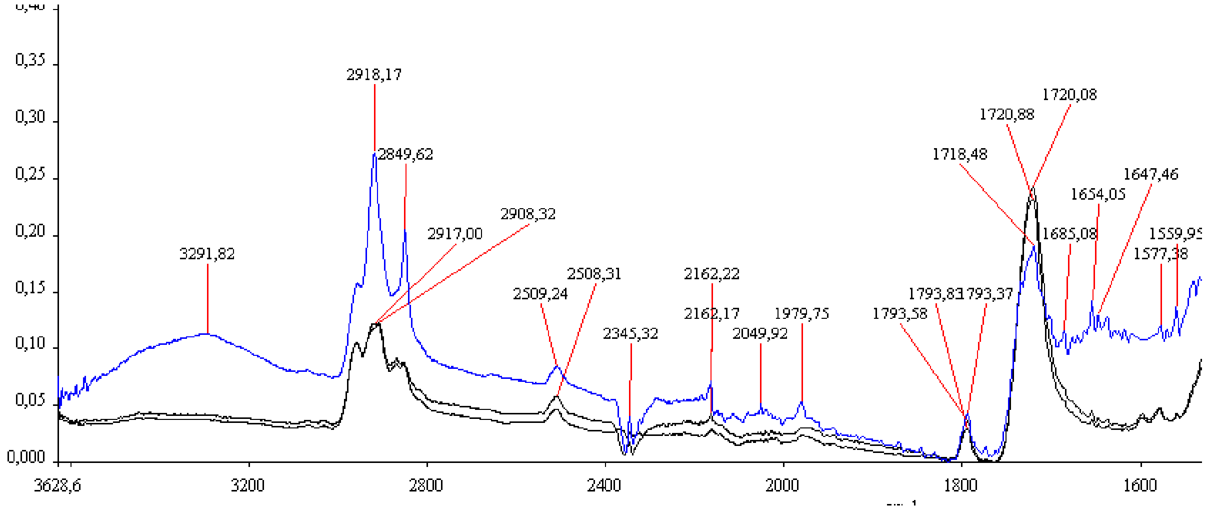

Figure 39. Normalized spectrum of B1. The NC (black), MC (black) and MCR (blue). Energy monitored 1241 >980 J.

4.3.4. **Colour testing**

The trend for all PVC-materials was that the colour became darker of longer curing times and higher temperatures. B3 was especially dark in case of the MCR sample. B2 and B3 are shown in order to illustrate how the colour impression is influenced by the colour difference, Figure 40 and Figure 41 .

Figure 40. Picture of B2, NC (left), MC, (middle) and MCR, (right)

Figure 41. Picture of B3, NC (left), MC, (middle) and MCR, (right)

Table 11. Results from colour testing, NC was the reference sample.

Sample	**Total colour difference (dE) from the average of the five measurement angles, 15 – 110 °**
B1 MC	32,1
B1 MCR	55,4
B2 MC	25,1
B2 MCR	44,4
B3 MC	57,1
B3 MCR	81,0
B4 MC	12,2
B4 MCR	17,5

4.3.5. Hardness testing

The hardness results are listed in Table 12. B1 displayed a larger increase in hardness between MC and MCR, than between NC and MC. The change between NC and MC was minor. There was a significant increase in hardness for B2. The increase in hardness for B3 was proportional for all three curing experiments. B4 exhibited a large variation of hardness values within each sample and thus causing difficulties in measurements.

Table 12. IRHD values for B1, B2, B3 and B4. (IRHD-micro, Shore D for the harder materials)

Experiment	**B1** **Shore D**	**B2** **Shore A**	**B3** **IRHD-micro**	**B4** **IRHD-micro**
Normal curing	50,2	85,2	48,6	66,5
Maximum curing	52,2	87	53,8	72
Maximum curing re-runs	59,4	89,8	57,6	73

4.4. Process verification

The hardness of the NC-specimens from the actual curing process was in close agreement with that of the oven simulated sample, showed in Table 13 which is satisfying. The hardness increased for every curing step in the curing process. In Table 14 the colour changes are shown, the NC samples cured in the process has darker colour than the experiments from the oven simulations.

Table 13. Hardness results from the process verification, B1 was measured with Shore A and B3 by IRHD

	1* 150 °C	**2* 150 °C**	**3* 150 °C**	**4* 150 °C**	**5* 150 °C**	**NC**	**NC oven simulations**
B2	84,2	86,6	86,6	87,6	88,8	86	85,2
B3	48,4	49,4	51,2	52	52,3	49,2	48,6

Table 14. Colour results from the process verification for B1 and B2

	1* 150 °C	**2* 150 °C**	**3* 150 °C**	**4* 150 °C**	**5* 150 °C**	**NC**	**NC oven simulations**
B2	1	19,8	26,8	30,2	30,8	6,9	1
B3	1	8,2	8,6	11,8	12,4	11,0	1

5. Discussion

In this section the theories and results are combined in order to draw conclusions from the measurements. The reliability of the characterization methods is discussed together with the accuracy of the results. The correlation between the DMTA results and the indicative methods is also investigated in order to make quick decisions regarding the quality during the car manufacturing process.

5.1. Polybutadiene-based materials E1, E2 and E3

The mechanical properties of E1 were retained for all three experiments. The increase in hardness between NC and MC can be a surface phenomenon which could be caused by oxidative reactions yielding a crusty surface layer. This was confirmed by the DMTA result which showed no difference in the mechanical properties of the material. The decrease in swelling for MC and MCR might result from crust surface layer. This phenomenon causes less absorption of solvent. This can be correlated to the DMTA results since there was no sign of increased crosslinking for the MC and MCR sample. FTIR measures the surface and there was a change in absorption between NC and MC, which also support the theory. The damping factor curve suggests a blend of rubber materials. Above about 60 °C measurements errors probably result in noisy data.

There was a change in the mechanical properties of E2 resulting from longer curing times and higher temperatures. The shift in T_g towards higher temperatures can be explained by a higher crosslink density. The damping modulus factor curve for NC sample had two peaks. When the curing proceeded longer they were combined into one peak, which can be a result of an increased crosslink density. The increased crosslinking contributes to the increased hardness and decreased swelling. The explanation for the significant increase in hardness is however mostly related to a crusty layer on the surface. For MC and MCR cracks were observed in the surface. FTIR data showed a higher amount of sp^3 carbons in the MCR samples' surface. The peak at 3004 cm^{-1}, representing sp^2 carbons, is present in the NC sample. The absorption was decreased for MC and MCR, due to consumed carbon double bonds in the vulcanization process. This also indicates a more crosslinked material and is according to the other results.

The ability to investigate the mechanical and chemical changes for different curing conditions with DSC in the manufacturing process can be successful when a more advanced equipment is used. The equipment should be sensitive and accurate in order to obtain T_g transition within the thermoset materials. Figure 25 shows a shift in T_g that can be correlated to the DMTA result for E2 shown in Table 4. T_g was increased for MC and MCR.

For E3 there were two distinct peaks in the damping factor, which might indicate the presence of two polybutadiene-based polymers with different T_g, this is however a speculation. The shift in T_g towards a higher temperature for the first peak can be explained by increased crosslinking within the network of the blends of the two polymers. The second peak exhibited a much smaller shift in T_g but the reduced damping confirms a more crosslinked material. The DMTA results can be correlated to the hardness and swelling since the largest difference was between NC and MC. The increase in crosslinking is smaller between MC and MCR due to a slower reaction rate and less reactants.

The TGA results showed that the ash content was relatively high for all three materials which can be explained by the high amount of fillers in the material. The result indicated that these thermal properties were the same in the three studied experiments. According to the TGA results, the initial step involving mass loss of unreacted vulcanization agents was small compared to the next step involving degradation of vulcanized polybutadiene. That indicates a small amount of reactive groups. This applies to E1, E2 and E3.

5.2. Epoxy-based material, E4

According to the DMTA result there was a thermally induced change in the material indicating that the curing process for epoxy was not complete after the NC and MC processes. The shift in T_g between NC and MC is referred to increased crosslinking. The significant difference between the storage modulus curves also supports the increased crosslink density. The MCR sample lost its flexibility. The shift in T_g made it hard and rigid at room temperature. The material is used as vibration dampener and the car should function in a temperature range from -40 to 60 °C. The damping was lower for MCR, which could affect the application use since it becomes hard and brittle at lower temperatures.

An important observation from the DMTA result was that initially the T_g was shifted towards a higher temperature and the damping factor decreased from NC to MC. Then from MC to MCR the main difference was a decreased damping. This phenomenon might be referred to consumption of reactants which slowed down the reaction rate. The hardness and the colour results could be correlated with the DMTA graph, since the increase was in the same range for all of the three characterization methods. There was no sign of thermal degradation since the FTIR result in Appendix IV, showed no increased absorption of water or carbon double bonds which was referred to the first occurring degradation mechanism together with chain scission. The curing process can possible continue a long time inside the car body.

5.3. PVC-based material B1, B2, B3 and B4

All the PVC-based materials showed different amounts of losses in solvent and plasticizer during the TGA-tests. In the order from NC to MCR, the amount of solvent and plasticizer left decreased. This was observed in the TGA results where the first loss in weight was higher for the NC condition. B1 had a higher mass loss for NC and MC compared to MCR. This result did not correlate with the DMTA results where the loss in damping modulus was supposed to decrease with decreasing solvent content. Since a lower amount of plasticizer gives lower flexibility within the polymer chain, the material becomes harder and stiffer.

According to Table 10 there was a decrease in damping factor from NC to MC but from MC to MCR it is increased. Since DMTA measure mechanical properties of the bulk material and not primarily take surface properties into consideration, the variation in the result is confusing. The T_g shift in B1 could also describe this phenomenon since the T_g was increased from NC to MC and then decreased from MC to MCR. The storage modulus was slightly higher for MCR than for MC and NC. This phenomenon can be due to the lower amount of plasticizer and solvent in MCR which indicates more closed packed polymer chains and decreased flexibility.

The present amine peak at 3291 cm^{-1} from the FTIR result for B1 indicates that a degradation mechanism starting in MCR. This absorption might be from an adhesion promoter, polyaminoamide, which started to migrate to the surface. Hardness testing showed a significant increase from MC to MCR. Observations from the samples were also that there was a sticky crust that covered the surface, the sample also had an unpleasant smell which is characteristic for the adhesion promoter polyaminoamide. The significant increase in hardness could be a result from the polyaminoamide that was observed in the FTIR result. This could also be explained by migration or degradation of other additives since a large part of the thermal stabilizers were consumed. The material is used in NVH. The increase in hardness was a surface phenomenon which might affect the application of the material.

The DMTA result for B2 indicated a significant shift of T_g when the curing condition time and temperatures were increased. From NC to MCR there was an increase in T_g from -17,8 to 0,5 °C. The increase in T_g refers to decreased flexibility of the polymer chain, which is a result of a high loss of solvent and plasticizer and continued gelatinization. This observation was also supported by the decreasing damping factor from NC to MCR. The TGA result illustrates how the loss of plasticizer and solvent varied for the three samples. The amount of released plasticizer and solvent was increased from NC to MCR. The result from TGA supports the result from the DMTA, where damping factor decreased in the same manner as the amount of plasticizer. The increase in hardness from NC to MCR also supports the other two results. The broadness in damping peak for B2 might be referred to a gelatinization reaction. Inhomogeneities could cause the broadness in the damping factor. Figure 40 shows the colour difference for B2. The increase in hue darkness of the material from NC to MCR was in line with the other methods. All the indicative analysis methods can be correlated to the DMTA curve.

The DMTA result for B3 indicates a small difference in damping factor from NC to MCR, which indicates a lower amount of solvent and plasticizer. This phenomenon can be explained by the more closed packed polymer chains within the material. The material was very flexible and the flexibility was maintained for each of the curing conditions. According to the TGA result there was a large amount of plasticizer and solvent in the material. The colour changes in the material started on the surface where conjugated double bonds possibly were formed. The exact mechanisms of the double bonds were not investigated, due to the confidential additives included in the material. The significant colour change on the surface could be interesting to investigate further. FTIR showed no differences in absorption spectra for NC, MC and MCR. During hydrochlorination polyenes are formed and they cause increased darkness on the surface. Already at low concentrations of double bonds a large colour change could be observed.

The DMTA result for B4 illustrates a shift in T_g for the three different samples. From NC to MCR the T_g was increased. This shift in T_g indicates a decreased amount of plasticizer and solvent in MCR which can be related to the TGA result. The damping factor decreased in order from NC to MCR and was caused by less flexible polymer chains. For the MC and MCR the samples have a hard surface with cracks, which indicates an initial degradation and could be caused by oxidative reactions.

5.4. Evaluation of characterization methods

The problem formulation for this project was to suggest a method for characterization of mechanical and chemical property changes. The challenge was to investigate materials that in some cases were covered by sheet metal or applied on curved surfaces. A summary of the possibility to see changes during the curing process is presented in Table 15.

Table 15. Summary of changes in the materials for each characterization method in order to correlate the results, NC is used as the reference value. Plus sign means an increase and equal sign means no change.

Sample	**DMTA (T_g)**		**FTIR**		**TGA**		**Hardness testing**		**Colour testing**	
	MC	MCR	MC	MCR	MC	MCR	MC	MCR	MC	MCR
E1	=	=	=	+	=	=	+	+	N/A	N/A
E2	+	++	+	++	=	=	+	++	N/A	N/A
E3	++	++	+	++	=	=	+	+	N/A	N/A
E4	+	++	=	=	=	=	+	++	+	++
B1	=	=	=	+	+	+	=	+	++	++
B2	=	+	=	=	+	++	+	++	++	++
B3	=	=	=	=	+	+	+	++	+++	++++
B4	+	+	=	=	+	++	+	+	+	+

The DMTA was used to study the viscoelastic properties of the materials and to determine the T_g and damping factor. The drawbacks of the analysis method are that surface effects are not measureable. The degradation process begins on the surface due to contact with air and cannot be characterized by DMTA. This could cause an increase in hardness. The rheometer demands a good quality of sample, bubbles in the materials or uneven sides of the sample affect the measurements. The measurements also were affected by the attachment in the clamps. During cooling especially the rubbery materials contracted, this was compensated by tightening of the screws before the temperature ramp started. This was done to avoid flutter in the material. The method was very useful for studying changes of crosslinking and T_g for the different cured materials. For all materials, triplets of each sample were produced. The temperature ramping demanded liquid nitrogen for cooling, this limited the number of performed measurements. For most materials doublets were performed with very high accuracy, see Appendix I. Differences can be caused by the attachment of the sample and bubbles in the material.

DSC only requires a small amount of sample and therefore fulfills the possibility to evaluate the quality of the material directly from the car bodies during the manufacturing process. The opportunity to cut of sufficient sample exists for all investigated materials to make a DSC analysis. Unfortunately, the experiment with the Perkin Elmer DSC 7 instrument was not successful and no conclusion can be drawn from the graphs. This can be explained from the high crosslink density and a more sensitive and advanced equipment was necessary to obtain the endothermic glass temperature transition. The opportunity to have Els Verdonck use a Q2000 at TA Instruments showed that DSC can be used as a fast indicative analyzing method during the manufacturing process.

The purpose was to use colour testing as a fast and indicative analyzing method. If the colour testing result can be correlated to the mechanical changes within the material it can be a very useful tool for a quick control in the process. Depending on the material position in the car body the colour testing can be limited. The spectrophotometer demanded a smooth surface with a diameter of approximately four cm. Therefore colour testing is not appropriate for all materials. Colour measurements were not possible for the weld-through sealants, due to their location. But there was a potential in measuring colour for some of the PVC-based materials. E4 and B3 cover large parts of the inside of the car body which made it possible to measure colour. But since there are irregularities on the covered area the spectrophotometer needs to be optimized in order to be used during the manufacturing process. The samples from the process verification were darker than the samples cured in laboratory ovens. This could be caused by dirt and smoke from the process ovens and should be taken into consideration.

TGA was used in order to study the thermal degradation of the investigated materials. There were no significant difference between the differently cured samples revealed by the subsequent thermal degradation, for the materials based on polybutadiene and epoxy. The method cannot be used as a quality control during the process. All the materials started to degrade at 300 °C, which is a temperature higher than in the process. The ash content for the PVC samples were not the same for NC, MC and MCR. That can be due to inhomogeneities in the material or that there was too much sample in the pans so the material was not fully combusted.

Hardness testing is a quick and easy method. For some materials there was a large variation in the IRHD values. This can be explained by surface defects and inhomogeneities. The measurements employ an indentor to penetrate the sample. If it hits the filler material the value can be higher than average. The opposite result would be achieved if there is a bubble in the sample. E1 and E2 had a large variation in both hardness testing and colour measurments. For the epoxy- and PVC-based materials the accuracy was high for both hardness and colour testing.

5.5. **Process verification**

The hardness result for the samples that were applied on the scrap car body corresponded to the normal cured oven simulation process. The ability to investigate the hardness directly from the car body is possible for B2 and B3 since they are applied to accessible areas. The hardness depends on the applied thickness. Therefore measurements for quality control should be done at critical places, where the layer is of suitable thickness. There was a steadily increase in hardness for every re-run in the sealer oven.

The process cured samples had a darker colour compared to the oven simulations which can be explained by dirt and volatiles compounds from other applied materials.

6. Conclusions

- There were no significant differences in the three experiments for the polybutadiene based material E1. The increase in surface hardness will probably not occur in the car body since the material is an antiflutter or hemflange adhesive applied between two metallic parts and has little contact with air.

- There was a change in mechanical properties for the MCR sample of E2. The crosslinking density was increased. The tighter crosslinked network in MCR indicates that the polymer chains was more closed packed and the interactions within the material were stronger. The significant increase in hardness was an effect of surface oxidation.

- E3 can possible be a blend of two polymers. From NC to MCR there was a more crosslinked network within the material. There was a significant change in mechanical properties between the increased curing conditions.

- The epoxy-based material E4 showed a major difference in mechanical properties due the chosen scenarios. The vibration damping ability was decreased for MC and MCR. The crosslinking process may possibly continue after the car is produced.

- Thermal degradation was initiated in the PVC-based material B1. The fact that the adhesion promoter was migrating to the surface indicates that thermal stabilizers within the material were consumed during MCR. The crusty surface might affect the NVH ability for the material.

- The roof-ditch sealant B2 exhibited a significant increase in T_g which refers to loss of plasticizer. This caused less flexibility in the polymer chains and a more close packed structure. B2 showed consistent results for all indicative analysis methods, when comparing the results to DMTA. The fact that B2 is applied on visible areas on the car body, gives the opportunity to use the material for guidance during a quality control.

- The only notable result for B3 was the increased darkness and hardness in the material for MCR. This observation can be valuable in the quality control of the car body during the manufacturing process.

- For B4 there was a shift in T_g together with a minor reduction in damping factor. The loss in flexibility can be associated with a lower amount of plasticizer. The placement in the car body makes it impossible to use the material as a quality control during the process. It is also worth mentioning that the samples in this project were partly cured in contact with air, this might have affected the results. The intention was to simulate an environment between two metal parts.

- The selective process verification indicated that the oven simulation corresponds to the car manufacturing process.

7. Future work

This study resulted in valuable information but additional investigations should be performed. In order to draw conclusions about the possible thermal degradation of the materials details of the composition of the materials are needed. This could be done by using a Soxleth extraction apparatus and further quantified by Gas Chromatography-Mass Spectroscopy, GC-MS. The possible blend content in E3 could be characterized by Size Exclusion Chromatography, SEC. The chemical structure could be obtained by H^1 and C^{13} solid-state NMR. For characterization of the thermal degradation of the PVC polymer, conductivity measurements could be performed in order to quantify the amount of produced hydrochloride gas.

The DSC was not successful when using Perkin Elmer DSC 7. TA Instruments investigated the three curing conditions for one material, E2, with a more advanced instrument, Q2000 DSC. By using this more sensitive equipment the T_g values can be obtained fast and by using a very small amount of material. Further work is necessary for obtain the ability to correlate the DSC results to the DMTA results for each material.

Within the process windows minimum curing conditions exist, this scenario should also be studied in order to avoid uncured materials. This can cause problems in the manufacturing process and should be investigated.

The properties of the materials to work as sealants and adhesives are not considered in this thesis. The effect on adhesion and shrinking should be investigated in order to define limit values for curing times and temperatures.

Within the body shop there might be a production stop for a longer time that is allowed in the process windows. It would be valuable to correlate the curing effect of the number of re-runs with the time and temperature a car body can stay in the oven for a longer time. The curing effect is different when the car body is cured for a longer time without cooling in between.

References

[1] Fröberg. P. *About Volvo Car Corporation 2007 – 2008;* (2008). [2011-10-31]. Available: https://www.media.volvocars.com

[2] Fröberg. P. *Volvo Car Corporation 2010*; (2011). [2011-10-31]. Available: https://www.media.volvocars.com

[3] *Top picks for commutes.* (2011). [2011-11-01]. Available: http://www.cars.com/go/criteriaSearch/lifestylecritieriasearch.jsp?styletype=Commuters,

[4] Graco. *Anti-flutter;* (2010). [2011-11-01] Available: http://www.graco.com/Internet/T_PDB.nsf/SearchView/Transportation-AutomotiveStamping

[5] Brent. S. A. *Plastics materials and processing*, 3rd edition. London; Prentice Hall. (2005)

[6] Bellander. M, et. al. Polymer engineering and science: *Crosslinking of Polybutadiene Rubber Without Any Vulcanization Agent*. Vol 38; issue 8, page:1254-1260. Sweden: Stockholm(1998)

[7] Bellander. M. Polymer engineering and science: *Crosslinking of Polybutadiene Rubber Without Any Vulcanization Agent- High Perssure Vulcanization*. Lic.avh. Sweden: Stockholm: Kungliga Tekniska Högskolan (1998)

[8] Engels. H.W, et al. Ullmann's Encyclopedia of Industrial Chemistry: Rubber, chapter 9: *Chemicals and Additives*. (2011)

[9] Walker. K. *Sulfur vulcanization of natural rubber for benzothiazole accelerated formulations: From reaction mechanisms to a rational kinetic model.* West Lafayette: School of Chemical Engineering, Purdue University. (2008)

[10] Pham. H. Q and Marks. M. J. Ullmann's Encyclopedia of Industrial Chemistry: *Epoxy Resins*. Texas: Freeport. Dow Chemicals (2005)

[11] Revocoat. *E4, Extrudable adhesive layer for vibration dampening in the paint-shop*. Technical data-sheet, (2005)

[12] Cowie. J.M.G and Arrigh. V. *Polymers: Chemistry and physics of modern materials*, third edition, New York, Taylor & Francis Group (2008)

[13] SureChem. *Rheology-Improving Adhesion Promoters for PVC Plastisols.* Patent no: 2004018543. (20040422)

[14] Beyler. C. L and Hirschler. M. M. Fire protection engineering: *Thermal Decomposition of polymers*, chapter 7. (2003)

[15] Green. M and Wittcoff. H. *Organic chemistry principles and industrial practice*. Page 73. Germany: Darmstadt. Wiley-VCH. (2003)

[16] Zeus. *Thermal Degradation of Plastics*, (2005). [2012-01-05]. Available: http://www.zeusinc.com/UserFiles/zeusinc/Documents/Zeus_Thermal_Degradation.pdf

[17] Gamed. H.R. Engineering with Rubber: How to Design Rubber Components*; Materials and Compunds,* chapter 2. USA, Ohio: Department of polymer science, The University of Akron. (2010)

[18] Moeller. H. W. *Process in polymer degradation and stability research*. New York: Nova Science Publisher. (2008)

[19] Pielichowsk. K and Njuguna. J. *Thermal degradation of polymeric materials*. Page 206. United Kingdom: Shropshire, Rapra Technology limited, (2005),

[20] Thermal Solution: *Determination of the Linear Viscoelastic Region of a Polymer using a Strain Sweep on the DMA 2980.* (2012). [2012-01-09] Available: http://www.tainstruments.com/main.aspx?n=2&id=181&main_id=415&siteid=11

[21] Pradyot, P. Dean's analytical chemical handbook: *Thermal Analysis,* chapter 15. USA: New York, The McGraw-Hill Companing. (2004)

[22] MacDonald, R. *Colour Physics for Industry,* 2nd edition. England: West Yorkshire, the society of Dyers and Colourists. (1997)

[23] Hoffman, G. *Cielab Colour Space.* (2009). [2012-01-15] Available: *http://www.fho-emden.de/~hoffmann/cielab03022003.pdf*

[24] CALCE. *Hardness testing.* (2001). [2012-01-15] Maryland: University of Maryland, Available: http://www.calce.umd.edu/TSFA/Hardness_ad_.htm

[25] Rubber hardness. (2000). [2012-02-22] Inspiratech 2000 Ltd, Available: http://www.materials.co.uk/rubber.htm

[26] Marzocca. A. J. & Garraza. A. L. (2009) *Material Properties: Evaluation of the polymer-solvent interaction parameter χ for the system cured polybutadiene rubber toluene.* Argentina: Ciudad Universitaria Buenos Aires

Appendix

In following section the results are presented for DSC, repeatability of DMTA, FTIR for the PVC based materials and hardness measurements.

Appendix I: Repeatability

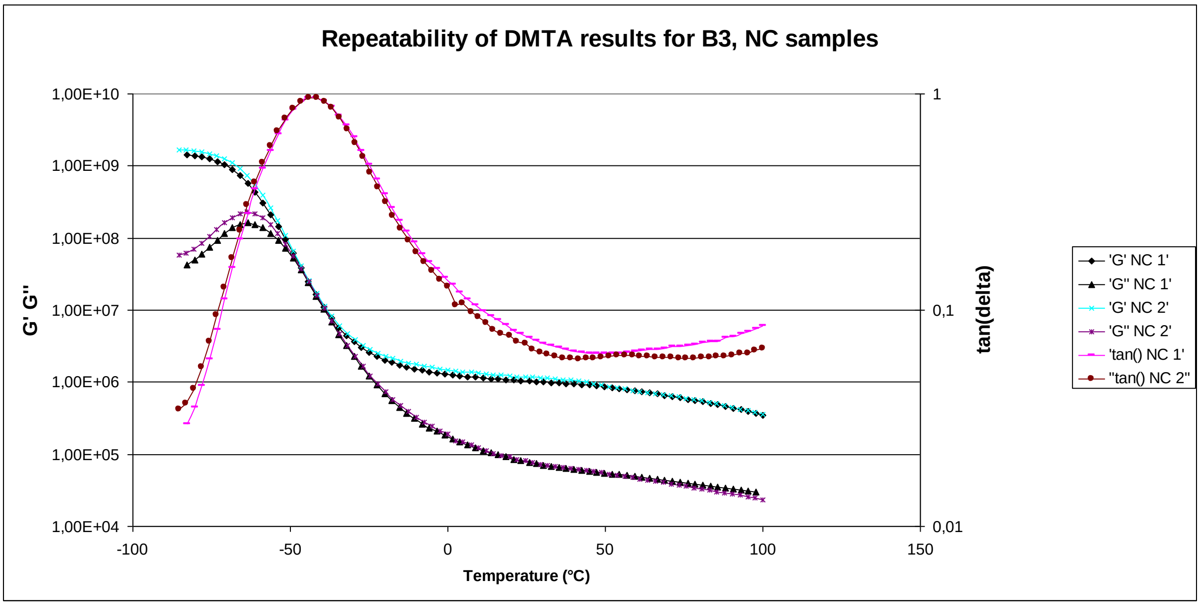

Figure 42. Repeatability results for DMTA

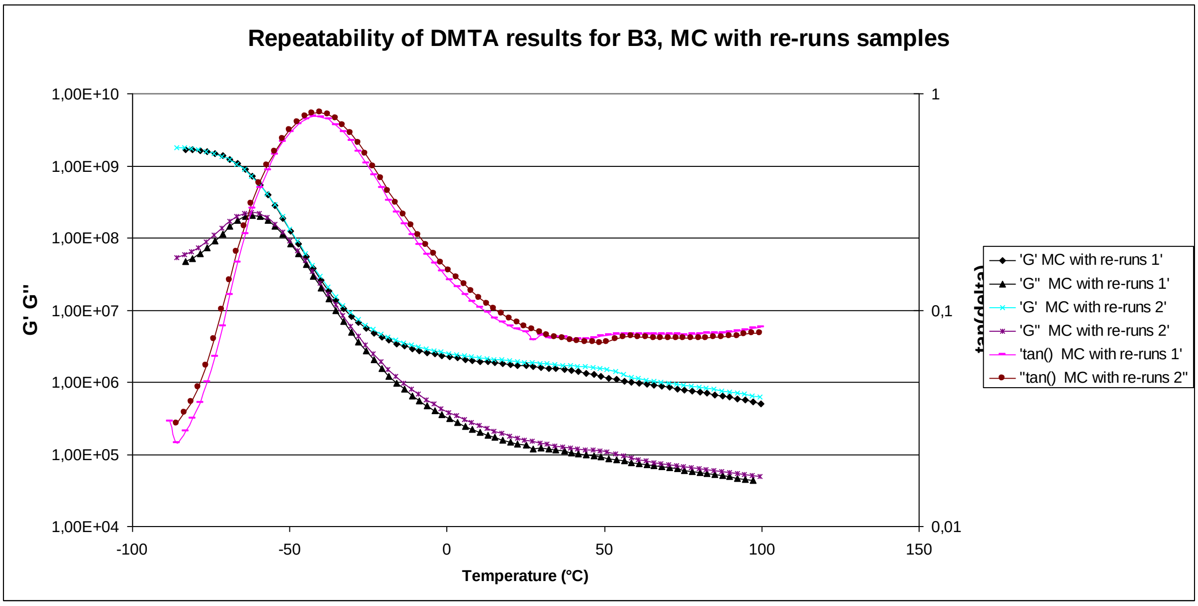

Figure 43 Repeatability results for DMTA

Appendix II: TGA temperature program

Temperature ramp 0-300°, 25 °C/min N_2 55,0 ml/min
Temperature hold 10 min, N_2 55,0 ml/min
Temperature ramp 300-800°, 25 °C/min, N_2 55,0 ml/min
Temperature hold 20 min, O_2 55,0 ml/min
Temperature ramp 800-900°, 25 °C/min, O_2 55,0 ml/min

Appendix III: DSC results

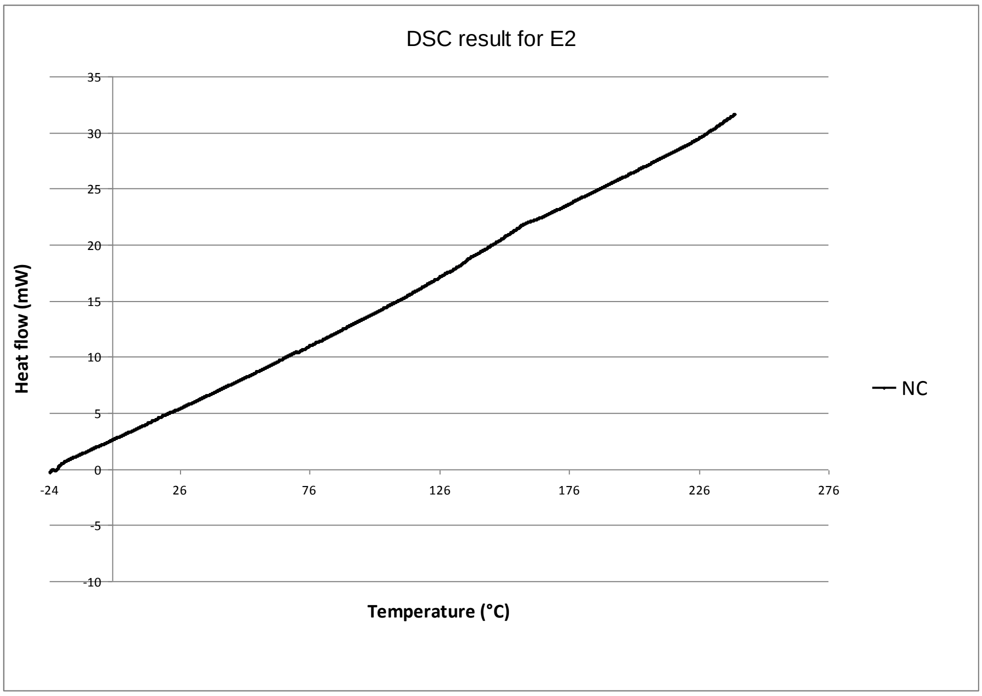

Figure 44. DSC result for E2, NC sample, temperature ramp from - 50.00°C to 240.00°C at 10.00°C/min. Nitrogen gas atmosphere.

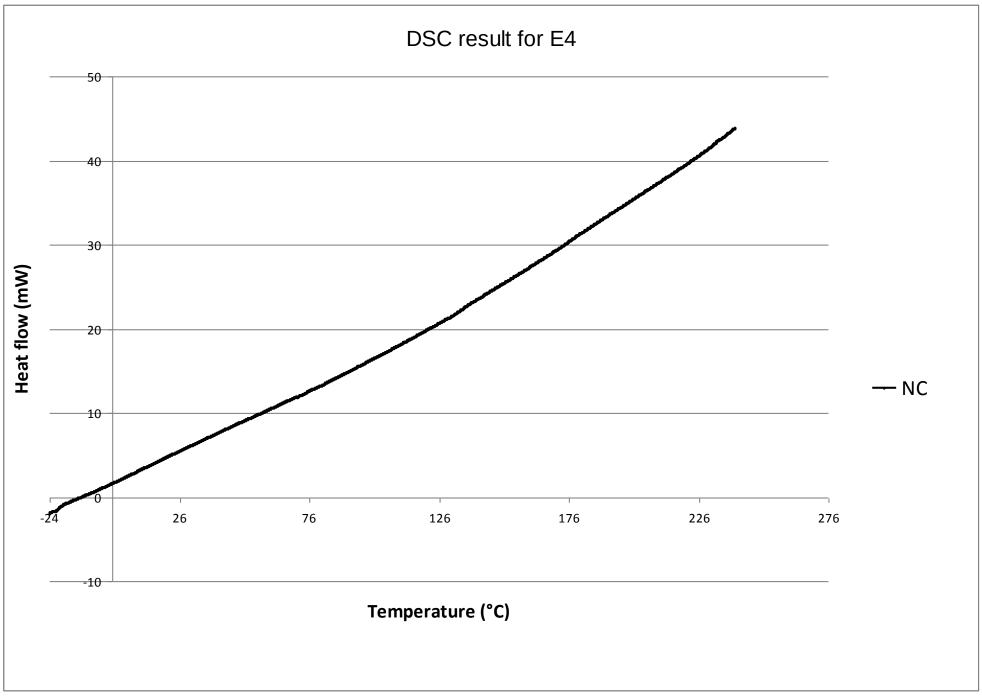

Figure 45. DSC result for E4, NC sample, temperature ramp from - 50.00°C to 240.00°C at 10.00°C/min. Nitrogen gas atmosphere.

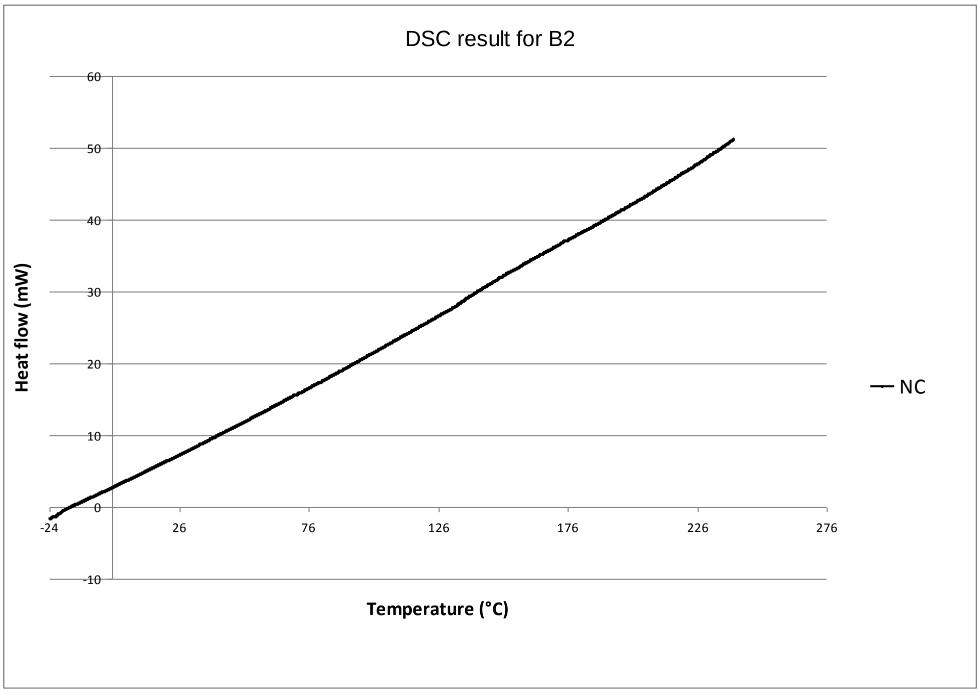

Figure 46. DSC result for B2, NC sample, temperature ramp from - 50.00°C to 240.00°C at 10.00°C/min. Nitrogen gas atmosphere.

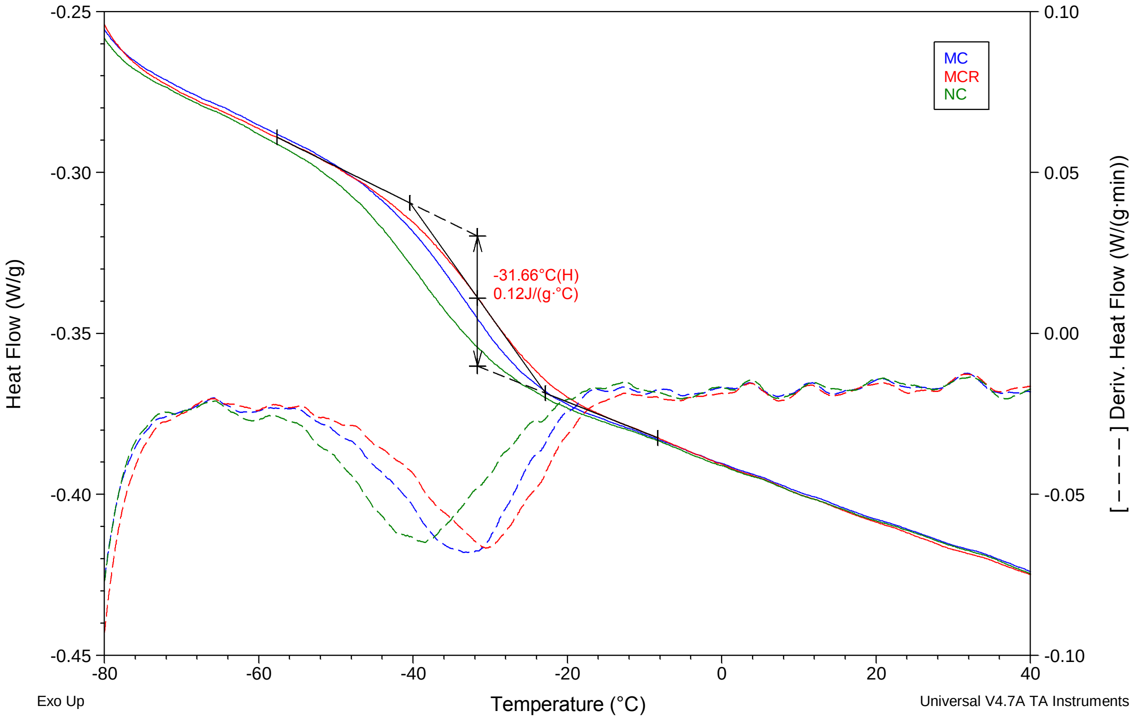

Figure 47. Illustration of the DSC results from TA instruments. Here the Tg is calculated based on inflection point for the NC (green) sample.

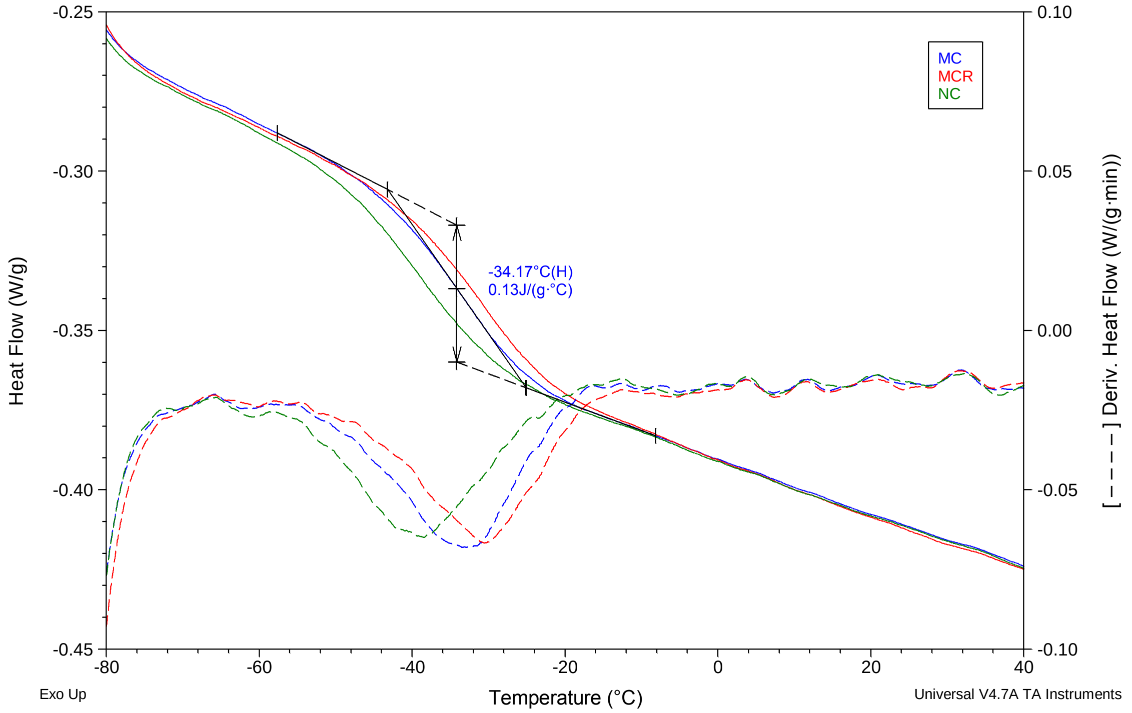

Figure 48. Illustration of the DSC results from TA instruments. Here the Tg is calculated based on inflection point for the MC (blue) sample.

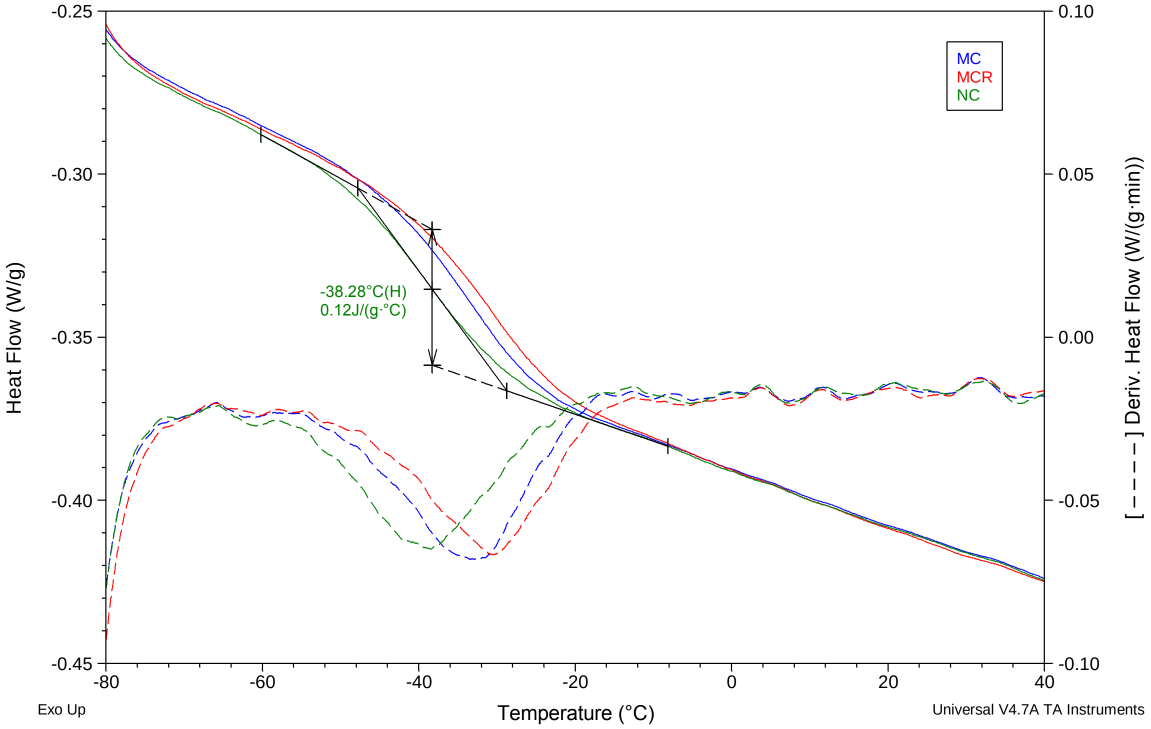

Figure 49. Illustration of the DSC results from TA instruments. Here the Tg is calculated based on inflection point for the MCR (red) sample.

Appendix IV: FTIR results

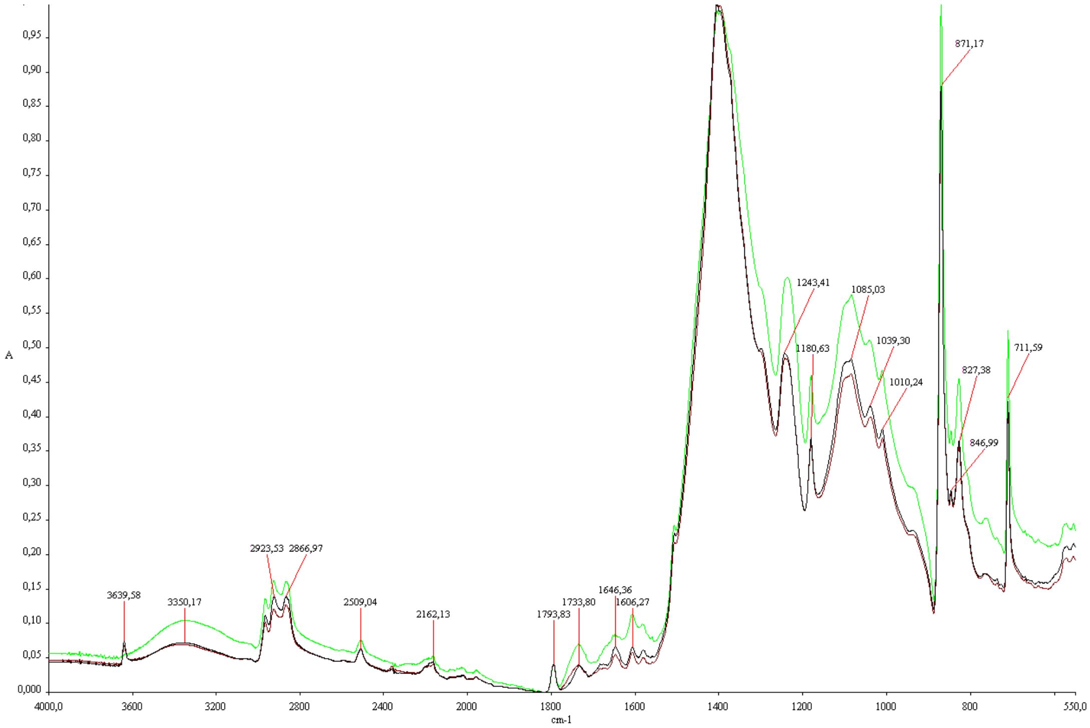

Figure 50. Normalized graph of E4. NC (blue line), MC (black line) and MCR (red line). Energy monitored 1242 >1057 J.

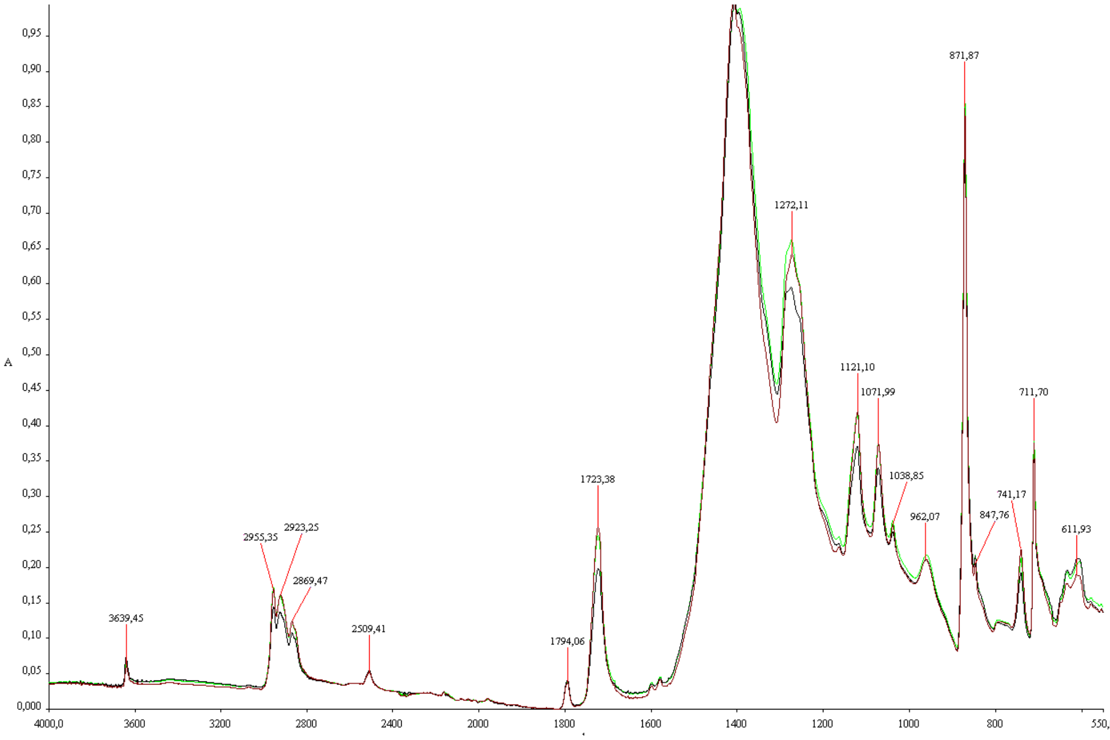

Figure 51. Normalized graph of B2. NC (blue line), MC (black line) and MCR (red line). Energy monitored 1242 >1057 J.

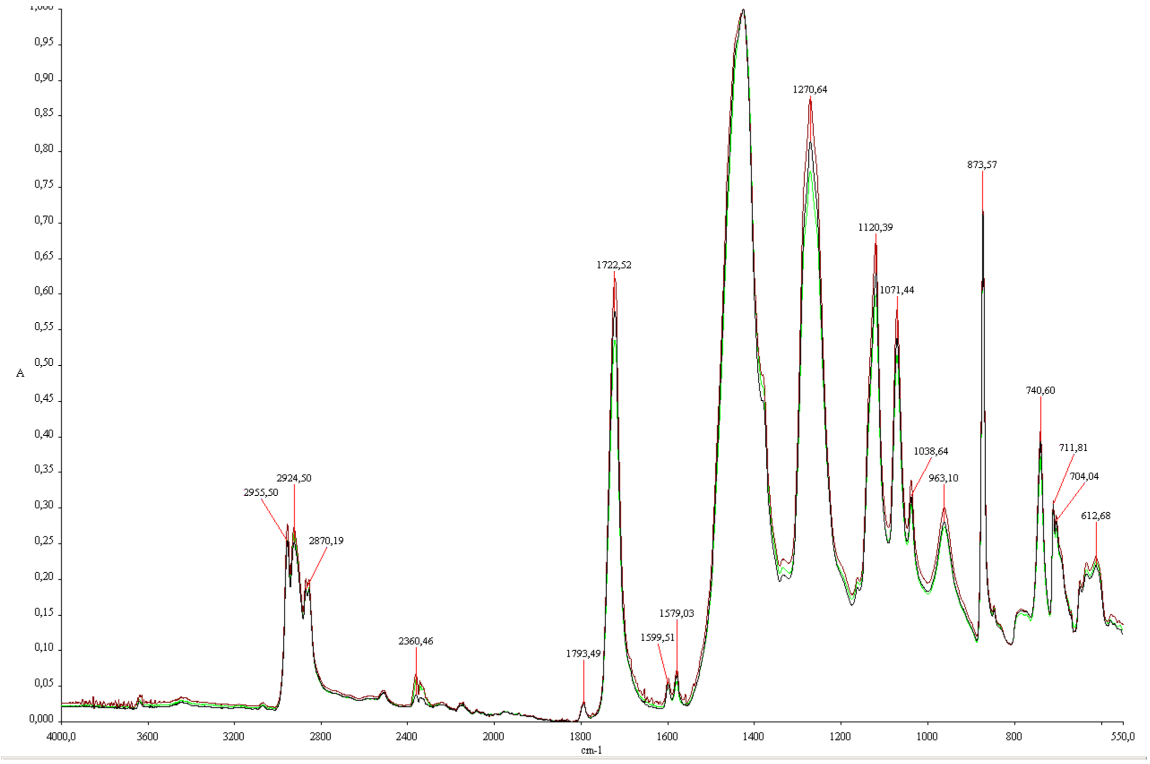

Figure 52. Normalized graph of B3. NC (blue line), MC (black line) and MCR (red line). Energy monitored 1242 >1057 J.

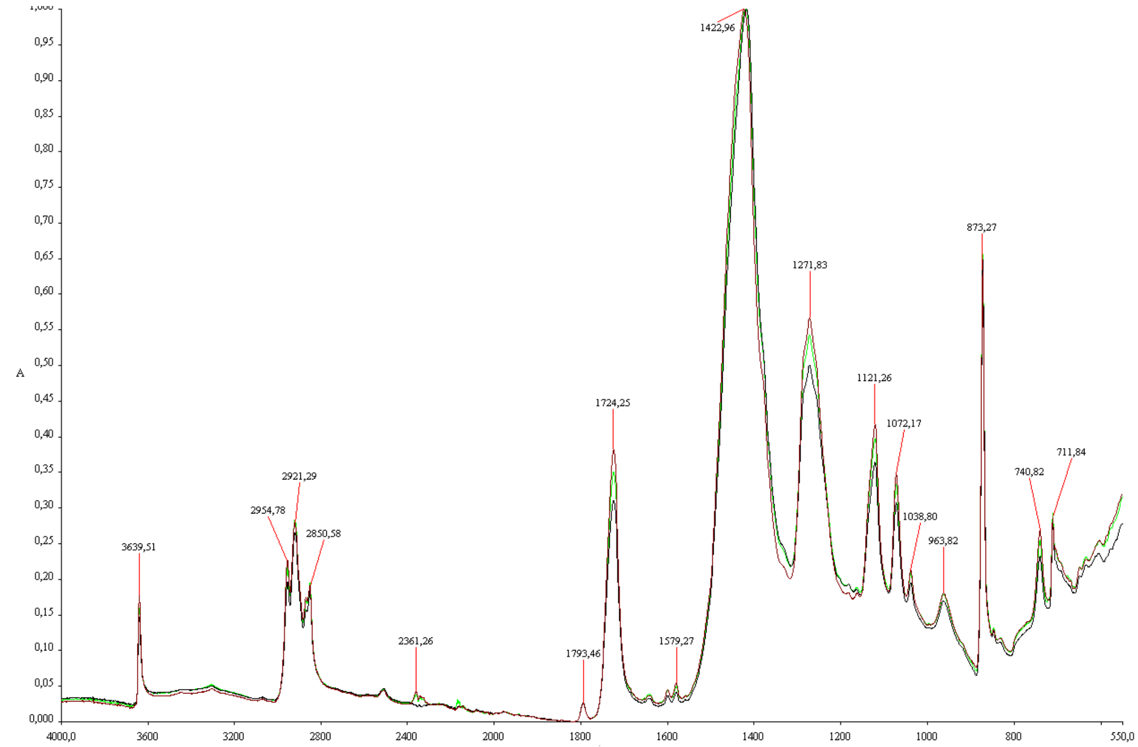

Figure 53. Normalized graph of B4. NC (blue line), MC (black line) and MCR (red line). Energy monitored 1242 >1057 J.

Appendix V: Colour testing

Table 16. Results from colour testing of polybutadiene materials, NC was the reference sample

Sample	**Total colour difference (dE) for the summation of the five measurement angles, 15 – 110 °**
E1 MC	23,1
E1 MCR	43,0
E2 MC	69,7
E2 MCR	23,1
E3 MC	16,9
E3 MCR	26,3

Appendix VI: Strain-sweep

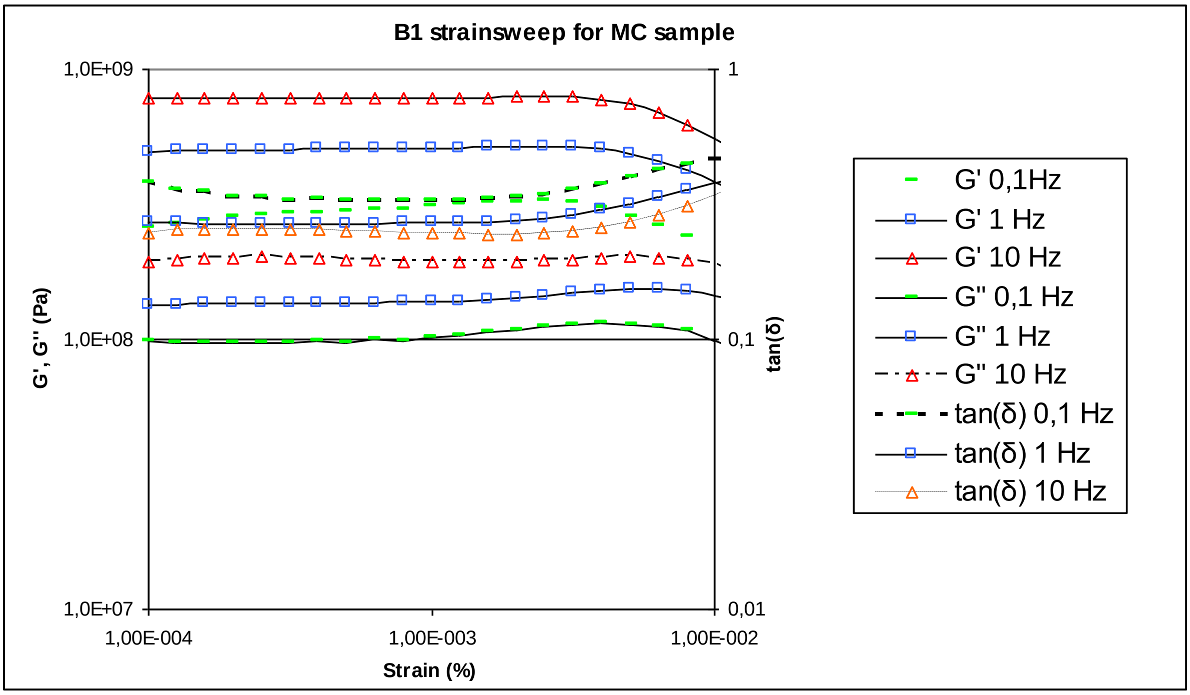

Figure 54. Strain-sweep of B1 for the MC.

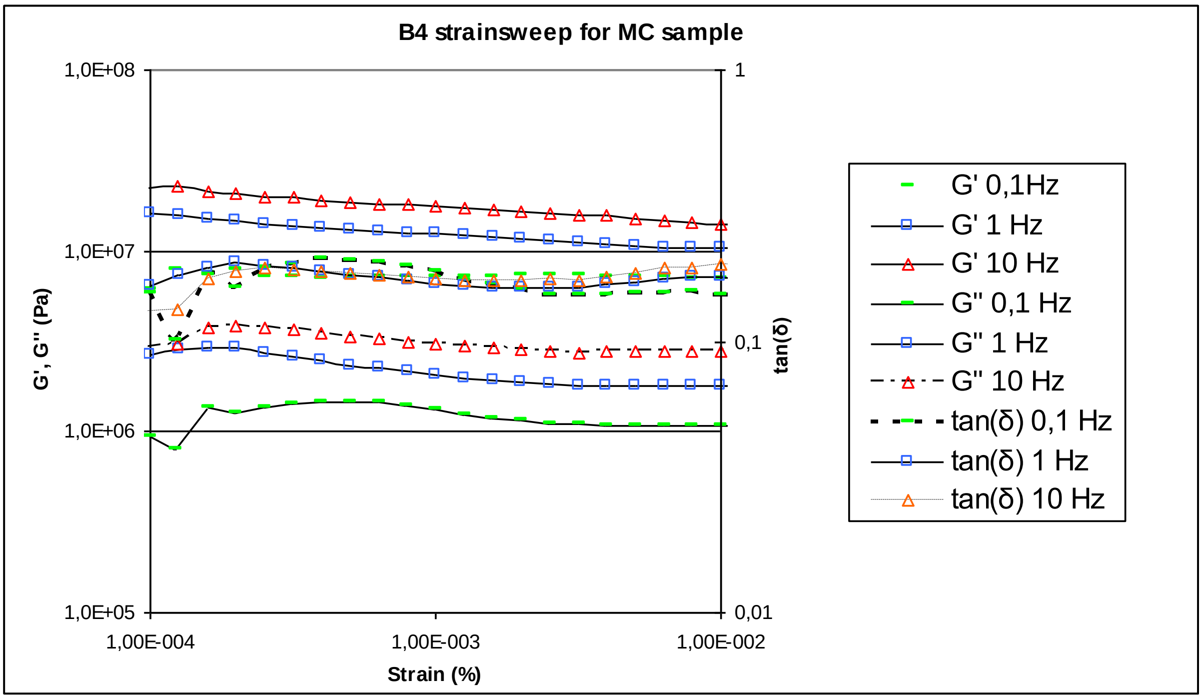

Figure 55. Strain-sweep of B4 for MC sample.

Appendix VII: Hardness results

Table 17. Hardness measurement for E1 using IRHD

E1 (IRHD)	**1**	**2**	**3**	**4**	**5**
NC	43	42	43	41	41
MC	48	47	50	49	49
MCR	51	49	48	48	50

Table 18. The hardness results for E2

E2 (IRHD)	**1**	**2**	**3**	**4**	**5**
NC	33	54	48	57	37
MC	62	57	61	61	62
MCR	75	77	81	74	79

Table 19. The hardness results for E3

E3 (Shore D)	**1**	**2**	**3**	**4**	**5**
NC	69	70	68	74	70
MC	72	73	70	70	69
MCR	69	69	68	70	69

Table 20. The hardness results for E4

E4 (Shore D)	**1**	**2**	**3**	**4**	**5**
NC	60	61	59	61	59
MC	67	70	70	66	69
MCR	74	79	72	75	75

Table 21. The hardness results for B1

B1 (Shore D)	**1**	**2**	**3**	**4**	**5**
NC	50	51	50	49	51
MC	52	53	50	53	53
MCR	60	60	57	60	60

Table 22. The hardness results for B2

B2 (Shore A)	**1**	**2**	**3**	**4**	**5**
NC	85	85	85	86	85
MC	88	88	86	87	86
MCR	90	91	90	89	89

Table 23. The hardness results for B3

B3 (IRHD)	**1**	**2**	**3**	**4**	**5**
NC	49	48	49	48	49
MC	54	52	54	54	55
MCR	58	58	59	56	57

Table 24. The hardness results for B4

B4 (IRHD)	**1**	**2**	**3**	**4**	**5**
NC	65	65	62	70	71
MC	70	73	74	72	71
MCR	72	73	73	74	73